NAVAL POSTGRADUATE SCHOOL

MONTEREY, CALIFORNIA

THESIS

A POSITION TRACKING SYSTEM USING MARG SENSORS

by

MIRYUNG UM

December 2007

Thesis Advisor: Xiaoping Yun
Second reader: Peter Ateshian

Approved of public release; distribution is unlimited

THIS PAGE INTENTIONALLY LEFT BLANK

REPORT DOCUMENTATION PAGE			*Form Approved OMB No. 0704-0188*
Public reporting burden for this collection of information is estimated to average 1 hour per response, including the time for reviewing instruction, searching existing data sources, gathering and maintaining the data needed, and completing and reviewing the collection of information. Send comments regarding this burden estimate or any other aspect of this collection of information, including suggestions for reducing this burden, to Washington headquarters Services, Directorate for Information Operations and Reports, 1215 Jefferson Davis Highway, Suite 1204, Arlington, VA 22202-4302, and to the Office of Management and Budget, Paperwork Reduction Project (0704-0188) Washington DC 20503.			
1. AGENCY USE ONLY ***(Leave blank)***	**2. REPORT DATE** December 2007	**3. REPORT TYPE AND DATES COVERED** Master's Thesis	
4. TITLE AND SUBTITLE: A Position Tracking System Using MARG Sensors			**5. FUNDING NUMBERS**
6. AUTHOR(S) Um, Miryung			
7. PERFORMING ORGANIZATION NAME(S) AND ADDRESS(ES) Naval Postgraduate School Monterey, CA 93943-5000			**8. PERFORMING ORGANIZATION REPORT NUMBER**
9. SPONSORING / MONITORING AGENCY NAME(S) AND ADDRESS(ES) N/A			**10. SPONSORING / MONITORING AGENCY REPORT NUMBER**
11. SUPPLEMENTARY NOTES The views expressed in this thesis are those of the author and do not reflect the official policy or position of the Department of Defense or the U.S. Government.			
12a. DISTRIBUTION / AVAILABILITY STATEMENT Approved for public release; distribution is unlimited			**12b. DISTRIBUTION CODE**

13. ABSTRACT (maximum 200 words)

The objective of this thesis was to further the development of a personal position tracking system using MARG sensors. This work advanced the method by which distance and heading were calculated of an individual wearing one MARG sensor on his/her foot when moving about under normal walking conditions.

Data was collected from the foot-mounted sensor while walking a straight-line path, a square path, and climbing stairs. The corresponding data from these activities was then used in a Matlab program to determine a computed position. The Matlab program employed a technique that reset the accelerometer error during the stance phase of the gait cycle. It also utilized a gait detection algorithm based on the magnitude of angular rate and the number of samples above/below threshold to establish the periods of the stance phase and the swing phase.

Experimental results from various testing scenarios showed that it is feasible to track position of a person.

14. SUBJECT TERMS MARG sensor, Gait Cycle, Quaternion, Angular Rate, Accelerometer, Magnetometer**,** Rotation matrix, Orientation, Earth Coordinate, Body Coordinate, Distance, Heading			**15. NUMBER OF PAGES** 77
			16. PRICE CODE
17. SECURITY CLASSIFICATION OF REPORT Unclassified	**18. SECURITY CLASSIFICATION OF THIS PAGE** Unclassified	**19. SECURITY CLASSIFICATION OF ABSTRACT** Unclassified	**20. LIMITATION OF ABSTRACT** UU

NSN 7540-01-280-5500 Standard Form 298 (Rev. 2-89)
Prescribed by ANSI Std. 239-18

THIS PAGE INTENTIONALLY LEFT BLANK

Approved of public release; distribution is unlimited

A POSITION TRACKING SYSTEM USING MARG SENSORS

Miryung Um
Captain, Korean Army
B.S., Korea Military Academy, 2002

Submitted in partial fulfillment of the
requirements for the degree of

MASTER OF SIENCE IN ELECTRICAL ENGINEERING

from the

NAVAL POSTGRADUATE SCHOOL
December 2007

Author: Miryung Um

Approved by: Xiaoping Yun
Thesis Advisor

Peter Ateshian
Second Reader

Jeffrey B. Knorr
Chairman, Department of Electrical and Computer Engineering

THIS PAGE INTENTIONALLY LEFT BLANK

ABSTRACT

The objective of this thesis was to further the development of a personal position tracking system using MARG sensors – miniature inertial measurement units comprised of magnetometers, accelerometers and angular rate gyros. This work advanced the method by which distance and heading were calculated of an individual wearing one MARG sensor on his/her foot when moving about under normal walking conditions.

Data was collected from the foot-mounted sensor while walking a straight-line path, a square path, and climbing stairs. The corresponding data from these activities was then used in a Matlab program to determine a computed position. The Matlab program employed a technique that reset the accelerometer error during the stance phase of the gait cycle. It also utilized a gait detection algorithm based on the magnitude of angular rate and the number of samples above/below threshold to establish the periods of the stance phase and the swing phase.

Experimental results from various testing scenarios showed that it is feasible to track position of a person using MARG sensors. Tracking accuracy remains to be improved in follow-up studies.

THIS PAGE INTENTIONALLY LEFT BLANK

TABLE OF CONTENTS

THIS PAGE INTENTIONALLY LEFT BLANK

LIST OF FIGURES

LIST OF TABLES

THIS PAGE INTENTIONALLY LEFT BLANK

EXECUTIVE SUMMARY

This thesis is a part of an ongoing effort to develop a system that brings real time human motion into a virtual environment using MARG (Magnetic, Angular Rate, and Gravity) sensors. This thesis has extended that research in several directions.

A new generation of inertial/magnetic sensors (3DM-GX1) from MicroStrain was used for this project. These sensors came with a library of functions written in the C language so that programmers could develop software to interact with the sensors.

The MARG sensor is composed of three orthogonal accelerometers, angular rate sensors, and magnetometers. This sensor is small and portable. Several experiments were conducted using this sensor, which was attached to the foot of a subject walking, under normal conditions. The data obtained from the MARG sensor were used to determine the distance and heading traveled by a person during a range of activities. Experiments were done with a person walking in a straight line of various distances and with two people walking a 48m straight line. Experiments were also done while a person walked in a circular and square path on a tennis court and in the lab, and while walking up a flight of stairs.

The X and Y components of angular rates were used to determine the phase of the human gait cycle. When a foot touches the ground, that phase is called the stance phase, and when a foot is swing through the air, that phase is known as a swing phase. During the swing phase, the X and Y angular rates exceeded a programmed threshold that allowed the determination of the swing/stance phase. The boundaries were then placed on the acceleration data. The acceleration data integrated over time was used to find the person's velocity over that step. However, the acceleration data had some errors, which was larger after integration for the velocity. Thus, the velocity was corrected for drift by subtracting the average of drift from the acceleration and zero velocity compensation. The initial velocity during a swing phase was assumed to be zero and the final velocity of swing phase was also assumed to be zero. It was further assumed that the drift was linear.

Thus, the linear drift was removed from the computed velocity to achieve more accurate velocity. The corrected velocity was integrated to determine the total displacement.

The data obtained from the sensor was in a body coordinate system. However, in order to track a human walking, the distance and position should be represented in an earth coordinate system. Thus, the data was transformed from the body coordinate system into an earth coordinate system. For the coordinate transformation, Euler angles or quaternions can be used. In this thesis, the quaternion orientation collected from the inertial/magnetic sensor was used to convert the body coordinate acceleration data into earth coordinates.

For circular or square walking paths, the estimated position was not correct because the measured angular rate also had drift. Thus the angle of heading was not correct. In order to obtain a more accurate tracking system, the heading was also corrected. When a person made a turn, the Z component angular rate would be changed because the person rotated about Z axis. The measured angular rates were integrated to determine the angles. However, the calculated angles from the angular rates had drift. Thus, the angles were corrected by subtracting the average of angles during stance phase from the original angles. Moreover, when a person paused at a same position for a while, the phase was determined as Initial phase, and then the angles were initialized to zero values.

Experimental results from various testing scenarios showed that it is feasible to track position of a person using MARG sensors. Tracking accuracy remains to be improved in follow-up studies

ACKNOWLEDGMENTS

I would like to express my gratitude to my thesis advisor Professor Xiaoping Yun for giving me the opportunity to work on this very interesting topic. I was interested in robotics and simulation systems. His dedication and efforts guided me through the development of this thesis and enhanced my learning experience at NPS.

Especially, I appreciate James Calsudian. He worked together to find the better results for this thesis and gave a lot of information to me.

To my husband Sanghyun, who makes me have great life and challenge, I would like to appreciate.

Finally, I would like to thank my parents for their love and support and to my heavenly father who has blessed me and continues to bless me in all things.

THIS PAGE INTENTIONALLY LEFT BLANK

I. INTRODUCTION

The MARG sensor project has undergone several iterations since 1994 at the Naval Postgraduate School. The sensor was used to integrate a humanoid into a network virtual environment [1]. After that work, several other projects have been accomplished involving the use of MARG sensors for orientation and position tracking - each project developing in the past works. This thesis is also based on the past works.

This chapter outlines the motivation, the goals and organization of this thesis.

A. MOTIVATION

Nowadays, the aspects of wars are very different from the past. Compared to past battlefields, it is getting wider and wider. In the past, the commander could see the whole battlefield at his position using his eyesight or a telescope because the battle was performed in one place. However, the present war has a wide battle field. For example, in the Iraq war, so many units were commanded and controlled in USA and the commanders wanted to see the movement of each unit or each soldier in their position in real time. Moreover, there were various obstacles which interrupted the ability to track the movement such as buildings, trees, or mountains. The important requests for strategic purposes are; "Where am I?", "Where are my friends?", and "Where is the enemy?" Thus, a position tracking system is very important for the military system.

Practically, the accurate real-time tracking of movement is widely used in applications of robotics, aerospace, underwater vehicles, automotive industry, virtual reality, and others. One of these systems is a Global Position System (GPS). If the application field is outdoors, then this system may be a tremendously powerful tool for this task. However, in indoor situations, GPS is unavailable, and so many researchers have attempted to develop a variety of systems, sensors, and techniques to find the location of a user. Practically, this indoor position tracking system is very useful in the real world. When a building was broken, using the position tracking system by cellular phones, many dead and wounded people were saved.

The most widely used system is a beacon system. Although this approach yields a high reliability, it is expensive in terms of installation and maintenance [2]. Another system uses visual equipment such as video and cameras.

In this thesis, instead of a vision system, a set of wearable sensors, which is based on the MARG (Magnetic, Angular Rate, and Gravity) sensors, are used to track the human position. The data collected from sensors need not be used for virtual environments either, but has other applications as well. Since these wearing sensors are small, they are able to be used anywhere. For example, if the soldiers who wear these sensors perform a mission or are trained, the commander could watch their movement. Moreover, in the real battle field, the commander will be able to track the troops, which carry out an operation indoors and save the wounded or locate dead soldiers. In addition, this system can be used in animation characters or humanoid robots. For instance, a human wearing these sensors can make a humanoid robot move to any location they wish and resemble their movement and to make an animation using a humanoid movement. Moreover, in the industry and medical fields, these sensors will also be useful. When the environment is very dangerous or sensitive, the humanoid robots will take the place of a human performance. LUO Yilun [3] used these wearing sensors for the digital writing instrument. Using the pen with the sensors, the letters could be shown on the monitor without any papers and ink. Because of these countless reasons, the research of this project is motivated and carried out.

B. GOALS

Hyatt Moore IV tried to make an accurate determination of the reliability of MARG sensors as a source-less position tracking device [1]. However, he developed an algorithm for off-line position tracking, and it can not be used in real time. The objective of this thesis is to develop an algorithm for tracking the position of persons using inertial and magnetic sensors and the data will be used in real time. Another objective is to develop a single algorithm that is able to reliably detect stance and swing phase of walking cycles for most test subjects. The final objective is to improve the heading estimation using the angular rate data to supplement magnetic data. Most of all, it is

important to obtain the best accurate algorithm that can be expected from the personal navigation based on use of inertial and magnetic sensors.

C. ORGANIZATION

This thesis is composed of five chapters as follows:

Chapter II provides information about human motion description and MARG sensor characteristics. In this thesis, the gait analysis is used to distinguish stance and swing phase. Thus this chapter provides the basic background about the gait cycle to determine the distance and the MARG sensor was used for this project.

Chapter III presents the mathematical models used for this thesis. It introduces the characteristics and notation of quaternions and shows how they can represent rotations and perform coordinate transformation.

Chapter IV is the core of this thesis. This chapter covers several experiments that were conducted using the sensors and sensor data collecting. These experiments were analyzed to determine the feasibility of using sensors to accurately estimate distance and heading of human movements.

Chapter V summarizes the work presented in this thesis with conclusions and recommendations for future work.

THIS PAGE INTENTIONALLY LEFT BLANK

II. BACKGROUND

A. HUMAN MOTION DESCRIPTION – GAIT ANALYSIS

Human gait pattern is different from that of animals which have four legs and each person has a unique gait cycle because of various walking styles depending on health states, personality, occupation, age, sex, lengths of legs, types of shoes, and many other attributes. Moreover, there are characteristic gait cycles following of walking, running, and stepping. The main concept of human walking is that as the body moves forward, one limb typically provides support while other limb is advanced in preparation for its role as the support limb. From the scientific research and analyzing about these various gait cycles, scientists are capable of producing robots which walk like humans and using these theories in many areas for human life such as the medical area.

1. Phase of the Gait Cycle

When people walk or run, people progress through three unique phases. The unique progress is called the gait cycle. In order to analyze the gait cycle, it is better to divide human walking into some parts because during walking, people repeat some motions. Through various methods to research these motion patterns, the gate cycle was able to be analyzed. One of these concepts is the theory of an American prosthesis by A. A. Mark, in which he divided the gate in eight contiguous phases (Figure 1). French physiologist, A. Marey, used a method similar to Mark's [4]. Since then, so many different theories, depending on authors' background, have been given to the world. However, this thesis will follow the description of Rancho Los Amigos Medical Center, in California [4]:

> The gait cycle in its simplest form is composed of stance and swing phases. The stance phase further is subdivided into 3 segments, including (1) initial double stance, (2) single limb stance, and (3) terminal double limb stance. The gait cycle starts and ends as a double stance, which means two limbs contact ground at same time. During walking, the gait cycle is composed of a single stance phase and a single swing phase. Single stance starts when the heel touches with the ground and ends when the toe leaves the ground.

Otherwise, a single swing phase means that the foot does not touch the ground. Each double stance period accounts for 10% of the gait cycle while single stance typically represents 40% (total 60%). The swing phase for this same limb is the remaining 40% of the gait cycle. At the swing phase, it is important to analyze velocity.

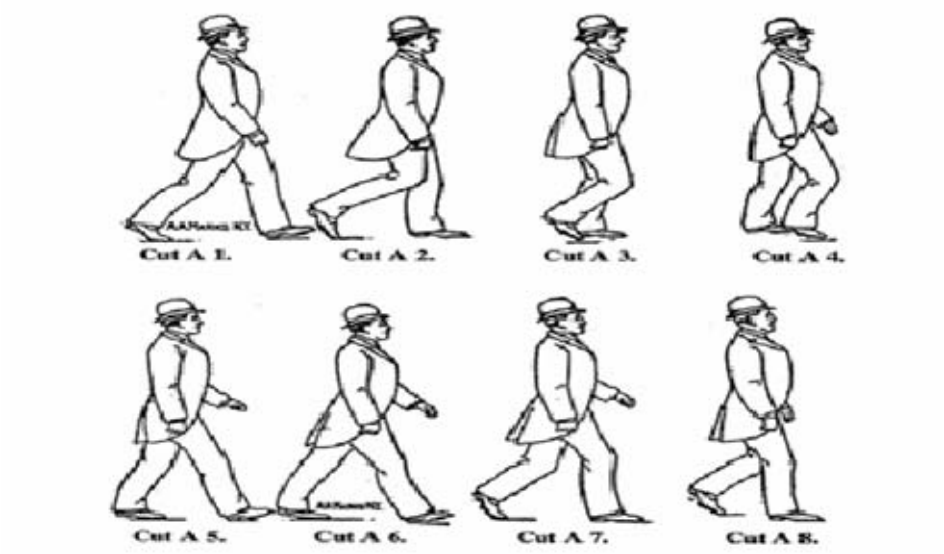

Figure 1. The Eight Contiguous Phases of the Gait According To A. A. Mark [From 4].

In summary, walking involves three main tasks.

- Weight acceptance (Double Stance)
- Single-limb support (Single Stance)
- Swing limb advancement (Swing)

2. Subdivision

Stance phase of gait is divided into four periods: loading response, midstance, terminal stance, and preswing. Swing phase is divided into three periods: initial swing, midswing, and terminal swing [5]. Figure 2 represents each period during the stance phase and Figure 3 represents each period during the swing phase.

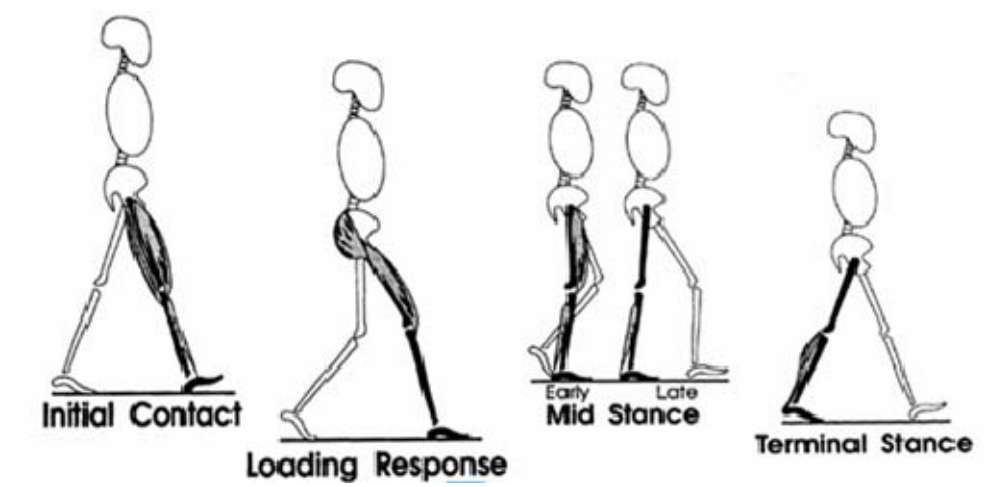

Figure 2. Divided Stance Phase [From 5].

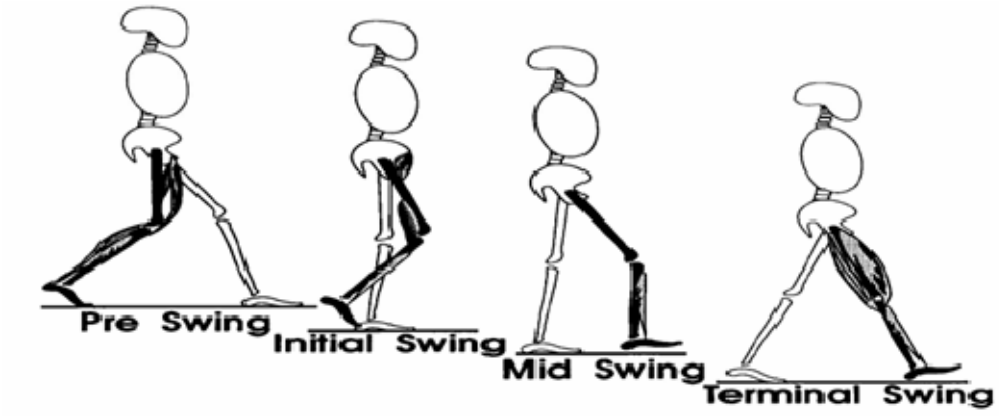

Figure 3. Divided Swing Phase [From 5].

During the stance phase, the initial contact means the instant the foot contacts the ground. The loading response begins at the initial contact and ends when the opposite toe leaves the ground. The midstance begins at the end of the loading response and finishes when the center of gravity is over the reference foot. The terminal stance begins when the center of gravity is over the supporting foot and ends when the opposite contacts the ground. At the terminal stance, the heel rises from the ground.

The preswing begins when the opposite is at the initial contact and ends at toe off. The period from initial contact to preswing composes about 60% of the gait cycle.

At the swing phase, the initial swing is the period from toe off to the maximum knee flexion (60 degrees). The midswing begins at the end of the initial swing and ends when the tibia is perpendicular to the ground. Lastly, the terminal swing phase begins when the tibia is vertical and ends at the initial contact. The stance phase is about 60 to 62% of the gait cycle and the swing phase is about 38 to 40% of the gait cycle and this is represented in Figure 4.

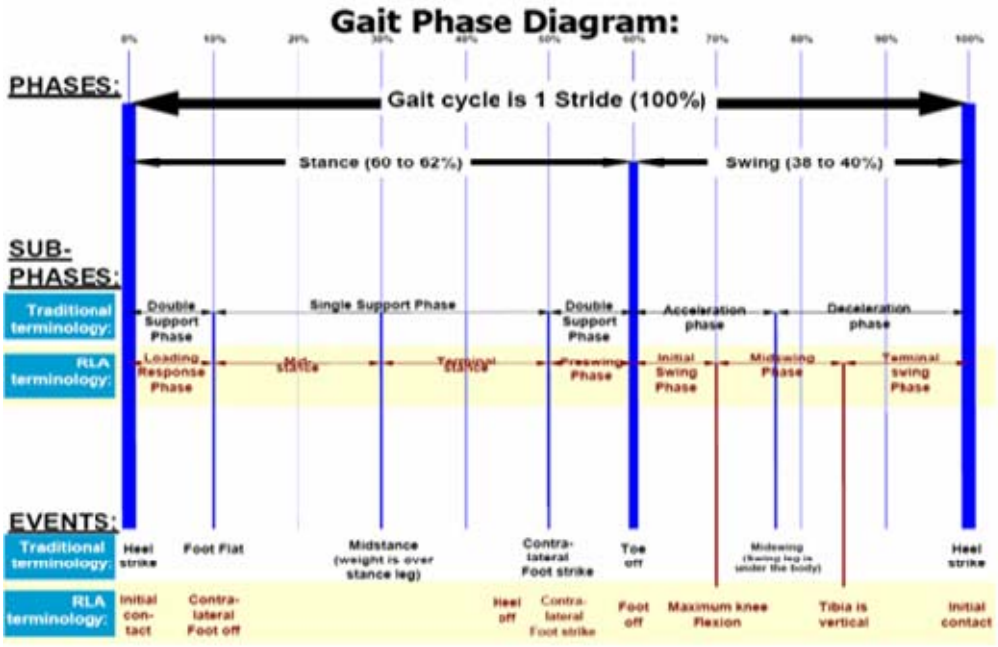

Figure 4. Gait Phase Diagram [From 4].

3. Distance of Motion

In order to calculate horizontal and vertical distance of human motion, it is important to understand determinants of gait. During walking, the center of gravity of the body makes a translation movement. The determinants of gait are composed of 6 components: variations in pelvic rotation, pelvic tilt, knee flexion at midstance, foot and ankle motion, knee motion, and lateral pelvic displacement in the transverse plane [6].

Among these determinants, the foot and ankle motions are the most important mechanisms because they contribute to keep the trajectory of the center of gravity in a horizontal position. The horizontal distance is estimated by using three dimensional acceleration of the subject's toe [7].

The horizontal distance is obtained by integrating the horizontal acceleration twice every step. During walking, the foot or toe have pitches, rolls and yaws changes. Via integrating acceleration during swing phase, horizontal distance is able to be obtained. It is necessary to estimate swing phase using an angular rate. From toe off to initial contact, the pitch angle is usually changeable. The angular velocity during the stance phase is almost steady. On the contrary, the angular velocity fluctuates during the swing phase. From Figure 5, each axis of the sensor attached on the foot is represented.

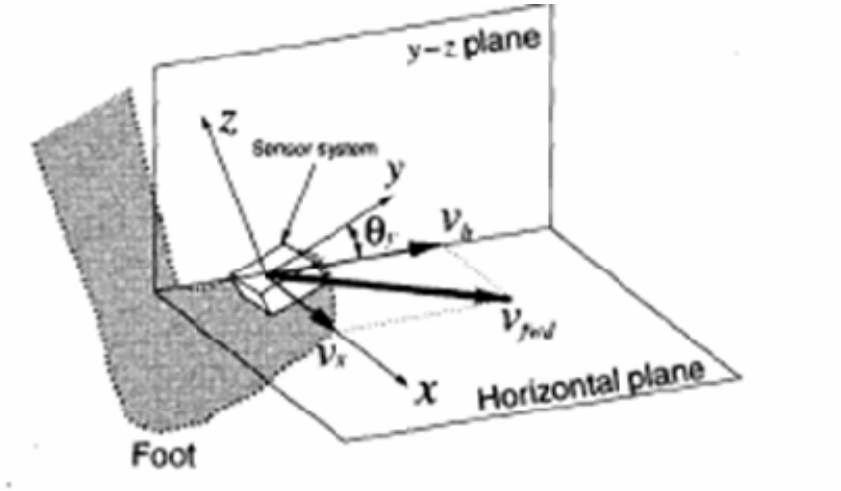

Figure 5. Estimation of Horizontal Velocity [From 7].

B. MARG SENSORS

In order to track the position in a virtual environment, a number of methods have been proposed. Mechanical, magnetic, optical, acoustic, or inertial methods are the examples to track the body movements. Among these methods, GPS is the most general method. A global positioning system tracks the position by measuring the distance between a GPS receiver and three or more GPS satellites. However, if the GPS signal is blocked by buildings, trees or vehicles, GPS will not be able to work to track the position. Therefore, tracking using MARG sensors can overcome these restrictions [1] [8]. These various methods have certain advantages and disadvantages, but for tracking the position without any sources like satellite, it should be self-contained and more accurate. Additionally, it should be smaller, portable, inexpensive and low power because it will be adhered to the human body to track the position.

For these reasons, the MARG sensor (3DM-GX1) is useful for these experiments to track the human position. Figure 6 is the front of the MARG sensor and Figure 7 is the inside of the MARG sensor.

Figure 6. 3DM-GX1 MicroStrain Sensor [From 9].

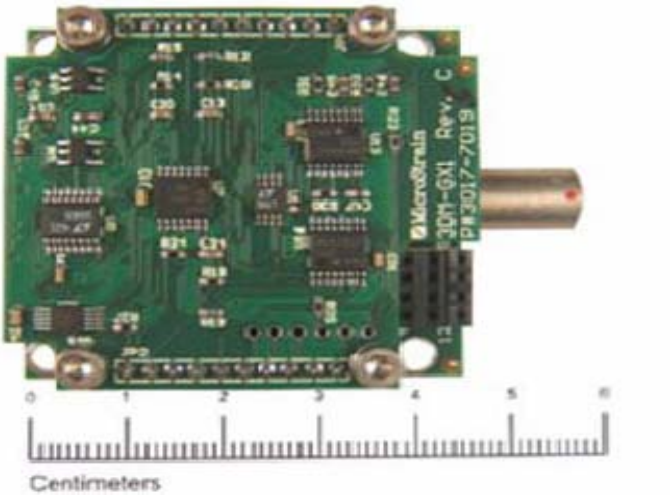

Figure 7. Printed Circuit Board(PCB) of MARG Sensor [From 1].

MARG sensors (3DM-GX1) consist of three angular rate gyros, three orthogonal DC accelerometers, three orthogonal magnetometers, multiplexer, 16 bit A/D converter, and embedded microcontroller. When the sensor is operated over the full 360 degrees of angular motion on all three axes, the sensor provides orientation in rotation matrix, quaternion, and Euler formats [9].

3DM-GX1 measures static and dynamic orientation. It utilizes the triaxial gyros to track dynamic orientation and the triaxial DC accelerometers along with the triaxial magnetometers to track static orientation. The embedded microprocessor contains a unique programmable filter algorithm, which blends these static and dynamic responses in real-time [9]. This sensor has a fast response about vibration and quick movements, while eliminating drifts and providing stabilized output. This stabilized output is helpful in eliminating unwanted jitter or noise from the read data [1]. The specification of the 3DM-GX1 sensor is listed in Table1.

	Parameter	Specification	Comments
Attitude	Range: Pitch, Roll, Yaw (°)	+/-90, 180, 180	No Attitude limitations
	Static Accuracy (°)	+/- 0.5	
	Dynamic Accuracy (° rms)	+/- 2	Typical, application dependent
	Repeatability (°)	+/- 0.2	
	Resolution (°)	0.1	
General Performance	A/D converter resolution (bits)	16	
	Turn on time (sec)	0.8	
	Analog output (Optional)	0-5V	4 channels, user configurable
	Update Rate (Hz maximum)	100	Orientation outputs
Physical	Size (mm)	65 x 90 x 25	With enclosure
		42 x 40 x 15	Without enclosure
	Weight (grams)	75	With enclosure
		30	Without enclosure
Electrical	Supply Voltage (V)	5.2 to 12 DC	
	Supply Current (mA)	65	
Environmental	Operating temperature (°C)	-40°C to +70	With enclosure
		-40°C to +85	Without enclosure
	Vibration (g rms)	4	20-700 Hz, white
	Shock Limit (unpowered) (g)	1000	
	Shock Limit (powered) (g)	500	
Communications	Serial Interface	RS-232, RS-485	RS-485 networking optional
	Serial Communications speed (kBaud)	19.2, 38.4, 115.2	User selectable
Angular Rate	Range (°/sec)	+/- 300	Custom ranges available
	Bias		
	Turn-on to turn-on repeatability (°/sec)	TBD	25°C fixed temperature
	In-Run stability, fixed temp. (°/sec)	0.1	After 15 minute warm up
	In-Run stability, over temp. (°/sec)	0.7	Over -40°C to +70°C range
	Short term stability (°/sec)	0.02	15 second Allan variance floor
	Angle random walk, noise (°/√hour)	3.5	Allan variance method
	Scale Factor Error (%)	0.5	Over -40°C to +70°C range
	Nonlinearity (% FS)	0.2	
	Resolution (°/sec)	0.01	
	G-sensitivity (°/sec/g)	0.01	With g-sensitivity compensation
	Alignment (°)	0.2	With alignment compensation
	Bandwidth (Hz)	30	-3dB Nominal
Acceleration	Range (g)	+/- 5	Custom ranges available
	Bias		
	Turn-on to turn-on repeatability (mg)	TBD	25°C fixed temperature
	In-Run stability, over temp. (mg)	10	Over -40°C to +70°C range
	Short term stability (mg)	0.2	15 second Allan variance floor
	Noise (mg/√Hz rms)	0.4	
	Scale Factor Error (%)	0.5	Over -40°C to +70°C range
	Nonlinearity (% FS)	0.2	
	Resolution (mg)	0.2	
	Alignment (°)	0.2	With alignment compensation
	Bandwidth (Hz)	50	-3dB Nominal
Magnetic Field	Range (Gauss)	+/- 1.2	
	Bias		
	Turn-on to Turn-on repeatability (mGauss)	TBD	
	In-Run stability, over temp. (mGauss)	15	Over -40°C to +70°C range
	Noise (mGauss/√Hz)	TBD	
	Scale Factor (%)	0.7%	
	Nonlinearity (% FS)	0.4	
	Resolution (mGauss)	0.2	
	Alignment (°)	0.2	With alignment compensation
	Bandwidth (Hz)	50	Nominal

Table 1. Detailed Specification of 3DM-GX1 [From 9].

In spite of these advantages, this sensor has some disadvantages. It is not useful for the laptop computer because the sensor can only be connected to the computer by a serial port. Nowadays, most computers have USB ports to connect external devices. Therefore, this sensor needs another device to switch this serial port into a USB port to get data from the sensor. Furthermore, it does not have an internal battery, therefore, it must be connected to the AC power or an external battery to supply power. In order to operate this sensor, extra connectors and external batteries should be connected like Figure 8. It doesn't look useful for moving and the sensor is not made for human body,

therefore it is more bulky. If this sensor is made smaller for human body and is modified to use a USB port for data communication, it will be more useful to track human position.

Figure 8. MARG Sensor with Peripheral Equipment for Operation.

C. SUMMARY

This chapter introduced the gait cycle and MARG sensors. This thesis uses the gait cycle concepts to determine the human position and the distance. It uses MARG sensors to obtain the data about accelerations, angular rates, and quaternions. In the gait cycle, walking involves three main tasks – initial stance, stance, and swing with each task being divided into some periods. In the case of stance phase, it is divided into four periods: loading response, midstance, terminal stance, and preswing. The swing phase includes initial swing phase, midswing phase and terminal swing phase. Through research about each period's characteristics, this project can determine swing, stance, and initial phase and then track the human position.

When a person wears MARG sensors during walking, these sensors can obtain the data through three angular rate gyros, three orthogonal accelerometers, and three orthogonal magnetometers. This sensor has advantages and disadvantages. However, while this sensor has some disadvantages, this sensor is very useful for this thesis because it is inexpensive, portable, and stable. It is able to be easily attached to anywhere on the human body and to offer the data we need.

III. COORDINATE TRANSFORMATION

In order to record the human position trajectory in real time, it is necessary to understand coordinate systems. The data obtained from the sensor is not represented in an earth coordinate system. It is represented in the body coordinate. Therefore, a transformation of coordinates will be used and quaternion will be used for the transformation.

A. ROTATION MATRIX

Any point in a three dimensional space can be located with a 3×1 position vector. However, there are various coordinate systems to represent the position including the earth coordinate system. In the MARG sensor application, the vector could be acceleration, velocity, angular rate and position in the three-dimensional space and each vector is represented in the body coordinate. However, the trajectory of the human position is usually represented in the earth coordinate. The coordinate transformation is performed using rotation matrices. As an example, the rotation matrix in equation (3. 1) corresponds to a single counterclockwise rotation through an angle α about the fixed Z axis.

$$P = \begin{bmatrix} \cos\alpha & \sin\alpha & 0 \\ -\sin\alpha & \cos\alpha & 0 \\ 0 & 0 & 1 \end{bmatrix} \qquad (3.\ 1)$$

In space, any orientation can be described as three sequential rotations by specified axis of the body frame and the angles of rotation are called the Euler angles [11]. For specifying an orientation X-Y-Z fixed angles, this convention is called roll (ϕ), pitch(θ), and yaw (ψ) angles. From multiplying each one-axis orientation matrix, the Euler angles for the rigid body orientation can be represented as one matrix.

- X-Y-Z Euler angles : $R(Z,\phi)R(Y,\theta)R(X,\psi)$ =

$$\begin{bmatrix} \cos\psi\cos\theta & \cos\psi\sin\theta\sin\phi - \sin\psi\cos\phi & \cos\psi\sin\phi\cos\phi + \sin\psi\cos\phi \\ \sin\psi\cos\theta & \cos\psi\cos\phi + \sin\psi\sin\theta\sin\phi & \sin\psi\sin\theta\cos\phi - \cos\psi\sin\phi \\ -\sin\theta & \sin\phi\cos\theta & \cos\phi\cos\theta \end{bmatrix} \quad (3.\ 2)$$

$$ {}^{B}_{E}R_{XYZ}(\phi,\theta,\psi) = \begin{bmatrix} r_{11} & r_{12} & r_{13} \\ r_{21} & r_{22} & r_{23} \\ r_{31} & r_{32} & r_{33} \end{bmatrix} \quad (3.\ 3)$$

Thus, the general form of orientation of fixed coordinate system is $P_E = {}^{B}_{E}RP_B$, where P_B is a vector in the body coordinate system and P_E is the corresponding vector in the earth coordinate system.

B. QUATERNION

In mathematics, quaternions are a non-commutative extension of complex numbers [10]. The quaternion representation of the rigid body rotation is:

$$q = q_1 i + q_2 j + q_3 k + q_0 = \overline{q} + q_0 \quad (3.\ 4)$$

Where $\overline{q}$ is the vector part, and q_0 is the real part of the quaternion.

In order to define an orientation motion, the rotation matrix and quaternion method can be used. However, usually quaternion can express the vector rotation much more compactly because the rotation representation by a quaternion uses 4 numbers and the representation of rotation matrix 9 numbers.

Converting vectors from one coordinate system to another can also be carried out using quaternion product as follows:

$$P_E = q \otimes P_B \otimes q^* = RP_B \quad (3.\ 5)$$

where q is denotes the quaternion product.

The rotation matrix is related to the quaternion components as follows:

$$R = \begin{bmatrix} (q_0^{\,2} + q_1^{\,2} - q_2^{\,2} - q_3^{\,2}) & 2(q_1q_2 + q_0q_3) & 2(q_1q_3 - q_0q_2) \\ 2(q_1q_2 - q_0q_3) & (q_0^{\,2} - q_1^{\,2} + q_2^{\,2} - q_3^{\,2}) & 2(q_2q_3 + q_0q_1) \\ 2(q_1q_3 + q_0q_2) & 2(q_2q_3 - q_0q_1) & (q_0^{\,2} - q_1^{\,2} - q_2^{\,2} + q_3^{\,2}) \end{bmatrix} \quad (3.\ 6)$$

IV. EXPERIMENT RESULTS AND ANALYSIS

A. PREPARATION

In this thesis, a MARG sensor is used for tracking the distance and heading of human walking. The MARG sensors provide the data about orthogonal angular rates, orthogonal accelerations, and quaternions. The experiments for this thesis are performed using these data from MARG sensors. However, these data are not accurate due to a number of reasons. If the distance or heading is calculated by the original data from sensors, the results will have some errors. Thus, this project investigates methods to correct the sensor data based on gait cycles.

The MARG sensor does not have an internal power to operate by itself and internal memory to save the data. To operate the sensor, 5 to 12 volts power is needed. However, during walking or stepping, the AC power can not be used because this sensor is attached to the human body. Thus, an external battery is used for this project. And to obtain the useful data, data obtained during the experiment should be saved. However a laptop computer is too big and heavy to handle. Thus, a smaller palm-top computer is used to save the data. Another disadvantage of this sensor is that RS-232 cable is used to connect a computer. Thus to use the palm-top computer, a RS-232 to USB converter is used.

To determine the gait cycle, this sensor is used to track the movement of a foot. Via the movement of the foot, it is able to track the human walking distance and heading. Thus, the sensor is attached to human instep of a foot. Moreover, if it is attached directly without any cushion to reduce vibrating or impact, the data will have more errors. Thus the sensor is fixed on a sponge tightly.

To obtain the 14 data (three components of acceleration, three components of magnetic field, three components of angular rate, four quaternions, sampling time), the Hyatt's code [1] was used. The 3DM-GX1 MARG sensors used in this thesis did not transmit wirelessly. Instead it had to be connected to a palm-top computer, and then the data could be transmitted wirelessly.

In order to access data from the sensor, Microstrain provided several functions written in the C language that developers could then incorporate into their own code [1]. For this reason, Hyatt made the algorithm written in C++ for the server so that the data could be polled from the sensors and then immediately sent to the client.

Figure 9 shows the MARG position tracking system worn by a user. Figure 10 and Figure 11 represent Hyatt's code GUI (Graphical User Interface) which is used to collect the sensor data in this thesis.

Figure 9. MARG Sensor Attached to a Foot and Connection with a Computer and Battery.

Figure 10. MARG Sensor Server GUI [From 1].

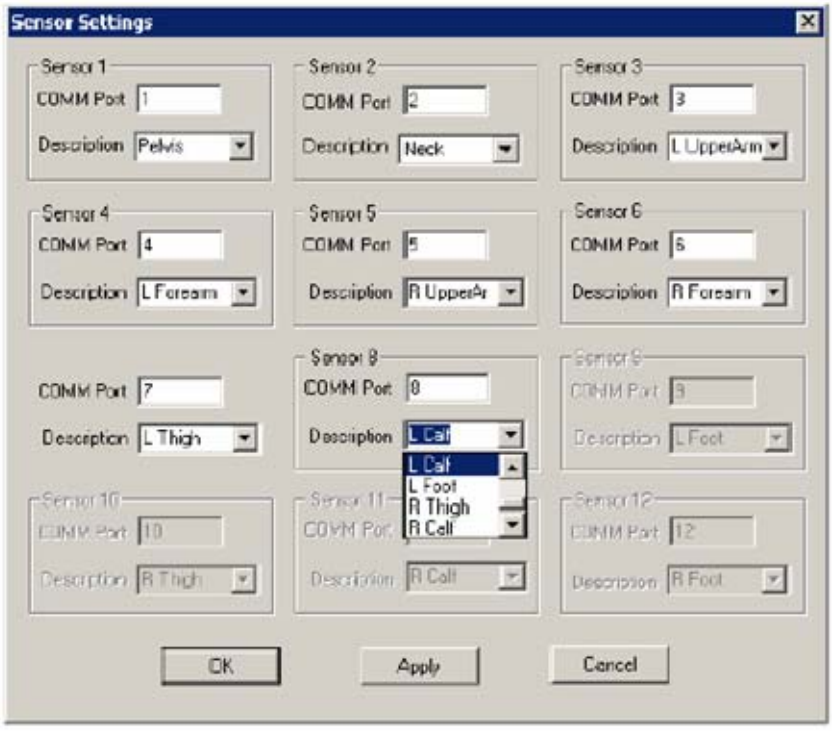

Figure 11. Server Setting Dialog [From 1].

B. DISTANCE

1. Introduction

In an effort to integrate a human being into a virtual environment, it is necessary to determine the human's change of position based on sensor readings. If a person wearing the sensor were to walk in some direction, the sensor data would give some information about direction and distance. However, the data are not exact. Sometimes, the data give the information that the person is walking to some directions when the person does not walk or does not change position. This section covers some basic topics on calculating displacement based on sensor data.

When some objects move from one position to another position, they have some information about acceleration, velocity and position. This information is related one to another. The distance that an object moves can be calculated by integrating over the object's velocity.

$$P(t_n) = \int_{t_{n-1}}^{t_n} v(\tau) d\tau \qquad (4.\ 1)$$

where $P(t_n)$ is the object's position at time t_n, $v(\tau)$ is the velocity at time τ in the range t_{n-1} to t_n. And range (t_{n-1}, t_n) is the period of integration, or the interval over which the velocity is being calculated [1]. The velocity can be expressed with relationship to acceleration in the following equation:

$$v(t_n) = \int_{t_{n-1}}^{t_n} a(\tau) d\tau \qquad (4.\ 2)$$

where $a(\tau)$ is the acceleration in the range (t_{n-1}, t_n). If the acceleration is known over a period of time, then it is possible to calculate an object's displacement from a known starting location. This sensor gives three orthogonal accelerations. Acceleration data is provided for the X, Y, and Z axis of the MARG sensor. Via these data, the position of human movement can be computed.

For human motion tracking, the human position is calculated from accelerometer data in real time. Unfortunately, the random noise and sensor bias in accelerometers will be accumulated and magnified due to double integration process [3]. Therefore, to correct theses problems, some feedback procedures are needed.

When the accelerometer measures three accelerations of X, Y, and Z axes, they have some drifts. The drifts will be represented as a constant value, ε, which has been added to the acceleration. The measured acceleration $a'(t)$ is represented as the true acceleration and drift.

$$a'(t) = a(t) + \varepsilon \tag{4. 3}$$

Thus, the measured acceleration will be integrated for the measured velocity, $v'(t)$. In this case, the drift is also integrated.

$$\begin{aligned} v'(t_n) &= \int_{t_{n-1}}^{t_n} [a(\tau) + \varepsilon(\tau)] d\tau \\ &= \int_{t_{n-1}}^{t_n} a(\tau) d\tau + \int_{t_{n-1}}^{t_n} \varepsilon(\tau) d\tau \end{aligned} \tag{4. 4}$$

Using Eq (4.2), the Eq (4.4) can be rewritten as $v(t_n)$ and drift $\varepsilon(\tau)$ is assumed as a constant over the interval (t_{n-1}, t_n).

$$\begin{aligned} v'(t_n) &= v(t_n) + \int_{t_{n-1}}^{t_n} \varepsilon(\tau) d\tau \\ &= v(t_n) + \varepsilon(t_n) \int_{t_{n-1}}^{t_n} d\tau \\ &= v(t_n) + \varepsilon(t_n) * (t_n - t_{n-1}) \end{aligned} \tag{4. 5}$$

To find true velocity, $v(t_n)$, the drift should be removed. For this purpose the drift has to be estimated. At interval (t_{n-1}, t_n), t_{n-1} represents the starting time that sensor is moved and t_n is the stopping time that sensor is paused, thus at the time t_{n-1} and t_n, the true velocities are assumed as zero values.

$$\frac{v'(t_n) - v(t_n)}{t_n - t_{n-1}} = \frac{v'(t_n)}{\Delta t} = \varepsilon(t_n) \tag{4. 6}$$

At the time $t = t_k$ between t_{n-1} and t_n, the drift $\varepsilon(t_k)$ can be rewritten by Eq. (4. 7).

$$\varepsilon_{t_k} = \frac{v'(t_n)}{\Delta t}(t_k - t_{n-1}) \tag{4. 7}$$

Thus, the corrected velocity at t_k is the difference between measured velocity and drift.

$$v(t_k) = v'(t_k) - \frac{v'(t_n)}{\Delta t}(t_k - t_{n-1}) \tag{4. 8}$$

In summary, these corrections can be represented by Figure 12.

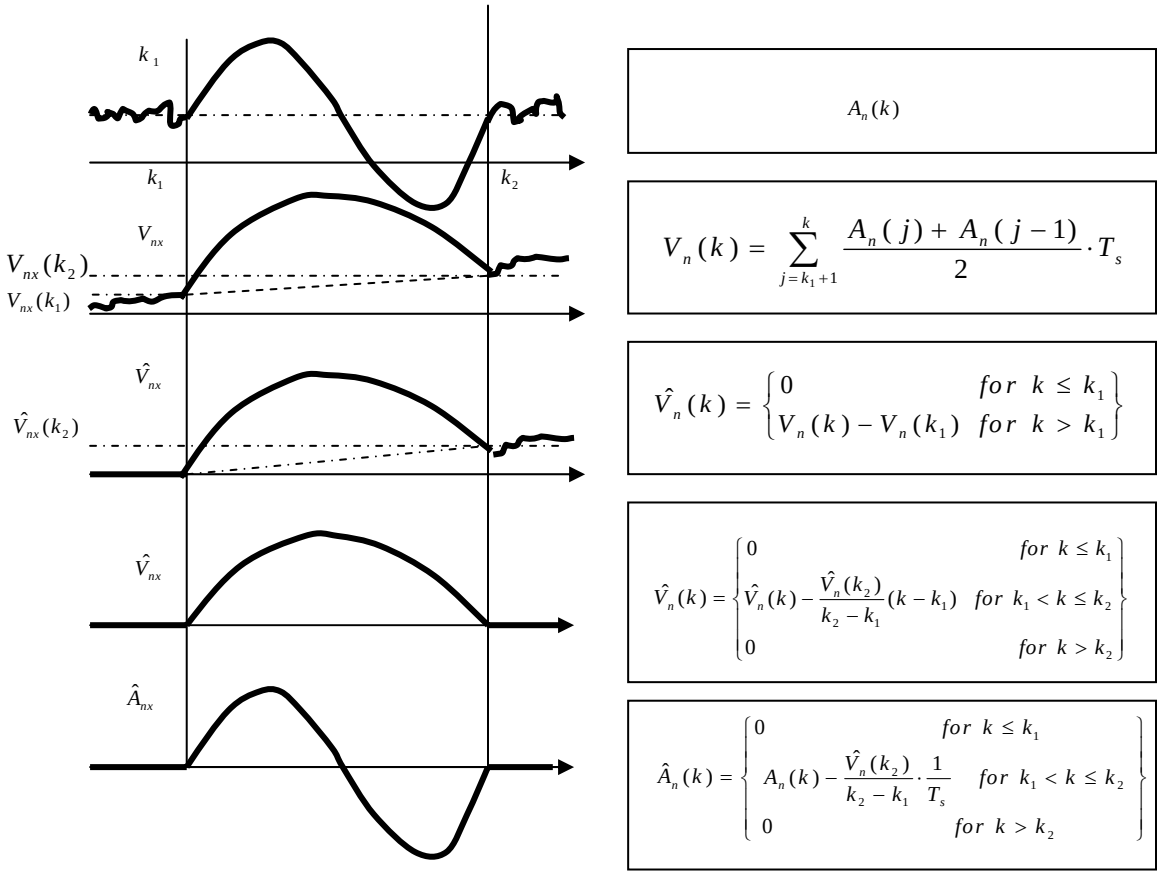

Figure 12. Zero Velocity Compensation [From 3].

2. Walking

a. Background

In Chapter II, walking is subdivided into 2 phases (Swing phase and Stance phase). This concept is very useful to track human walking. The stance phase consists of the period of time that it takes for a foot's heel to touch the ground until the time its toe leaves the ground. The swing phase begins at the point in time when the toe leaves the ground until its heel strikes the ground again [1]. Thus during swing phase, the foot is in the air and during stance phase, the foot touches the ground. The position is changed when the foot repeats swing phase. It means that the distance increases when the foot is swinging through the air and when the foot touches the ground, the distance is kept constant.

Data was obtained from only one sensor placed on the foot to determined the distance during walking. If the swing phase and stance phase are determined from the given data, the distance will be able to be calculated but it will be necessary to correct some errors because the measured data has a drift.

b. Coordinate Systems

The MARG sensor has a body coordinate system, but human position can not be computed through the body coordinate systems. In this analysis of the MARG sensor, two coordinate systems were used: Earth coordinates and Body coordinates. For example, the X-axis at the earth coordinates points toward the North Pole, while Z-axis points to the center of the earth, and the Y-axis points east [1]. However, The MARG sensor's body coordinates do not point the same direction of the North-East-Down coordinate systems. On the contrary, it is related to the foot. In order to track the human walking and determine the traveling distance, the body coordinates are transformed into earth coordinates.

The data from the sensor includes the information to transform the body coordinates into earth coordinates. The necessary quaternion can be computed from raw data. On the other hand, the quaternion can be provided by the MARG sensor itself.

Although the second method took slightly more time, it was a considerably easier approach. Using quaternion obtained from the MARG sensor, the body coordinates can be converted into earth coordinates via Eq.(3.6). Thus, the raw data (accelerations and angular rates) was converted into earth coordinate systems.

As a matter of fact, this conversion can also be performed using Euler angles and these angles can be obtained by the MARG sensor itself. However, if these data were used for transform processing, it would have some disadvantages such as a singularities.

However, in the code supplied by the Microstrain controller, some errors were found. The documentation for the source code [11] along with the comments in the source code both specified that there was no method for retrieving stabilized quaternion data and raw sensor data at the same time [1]. A separate communication document [12] supplied by Microstrain explained that it was possible to recover both stabilized quaternion data and raw data at the same time.

c. Gait Cycle Locator

After doing conversion of body coordinate into earth coordinate, it needs to determine gait cycle. When a person walks for some distance, walking cycle repeats stance and swing phases. In order to determine the swing and stance phases, it is necessary to analyze the motion of the foot during walking. In this thesis, the angular rates were used to determine the gait cycle.

Initially, a person keeps in a standing position for a while and then moves the foot forward to walk. The pausing period for starting the gait cycle is called the initial phase. The period of moving the foot in the air is called the swing phase. During this step, the angular rates would be changed. On the other hand, when the foot touches the ground, the foot does not move and it just stays at the same position. This period is the stance position. During this period, the angular rates would be changed a little bit.

Thus, if the angular rates are considered for the gait cycle, the position of the human will be determined because the distance increases during swing phase.

Figure 13 represents the angular rates of an eight meter straight walk in X, Y, and Z axes. A threshold may be applied to determine gait cycles. However, the angular rate profile is different from one person to another. A different threshold needs to be determined for each person.

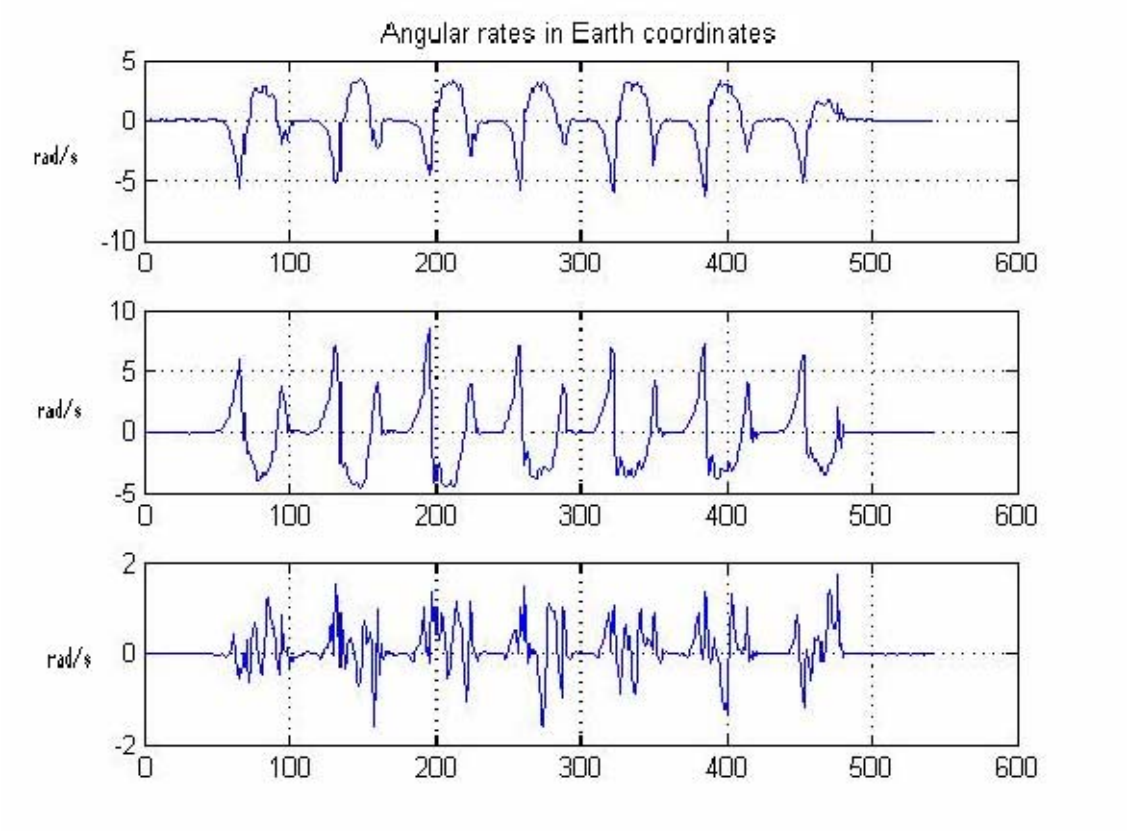

Figure 13. Angular Rates in Earth Coordinates (X-axis unit is the number of samples and Y-axis unit is radians per seconds).

For example, James and I did this experiment in the same location and at same time. However, for the best result, James's angular rate threshold was 0.35 and my angular threshold was 0.5. Furthermore, if the experiment was done in a different place and at a different time, the angular rate threshold could be changed little bit.

Figure 14 represents the length of angular rates of X and Y axes. If the length was greater than 0.5, it was determined as swing phase. The data inside the rectangle windows mean the swing phase. The number of rectangle windows means the step counts of walking. Thus, in this case, there were 7 steps for 8 meters.

From this figure, some errors could be found. The swing window leaned to the right side thus the more accurate data during swing phase could not be collected. The process of shifting the windows was needed. First, the raw data of accelerations were saved and then the prior 5 values of accelerations were saved. Then the acceleration data was replaced using the first value of the prior data. Thus, the acceleration window was shifted toward the left side by 5 indices. Figure 15 represents each acceleration after shifting the window toward the left side.

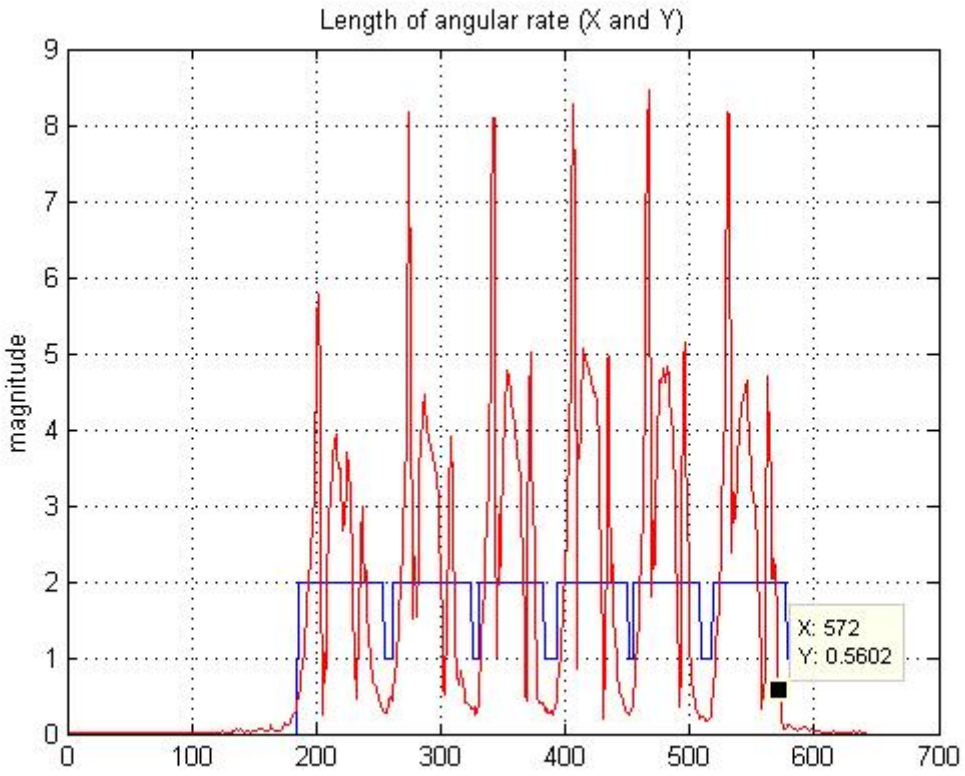

Figure 14. Determining the Swing and Stance Phases (X-axis unit is the number of samples and Y-axis unit is radians per seconds).

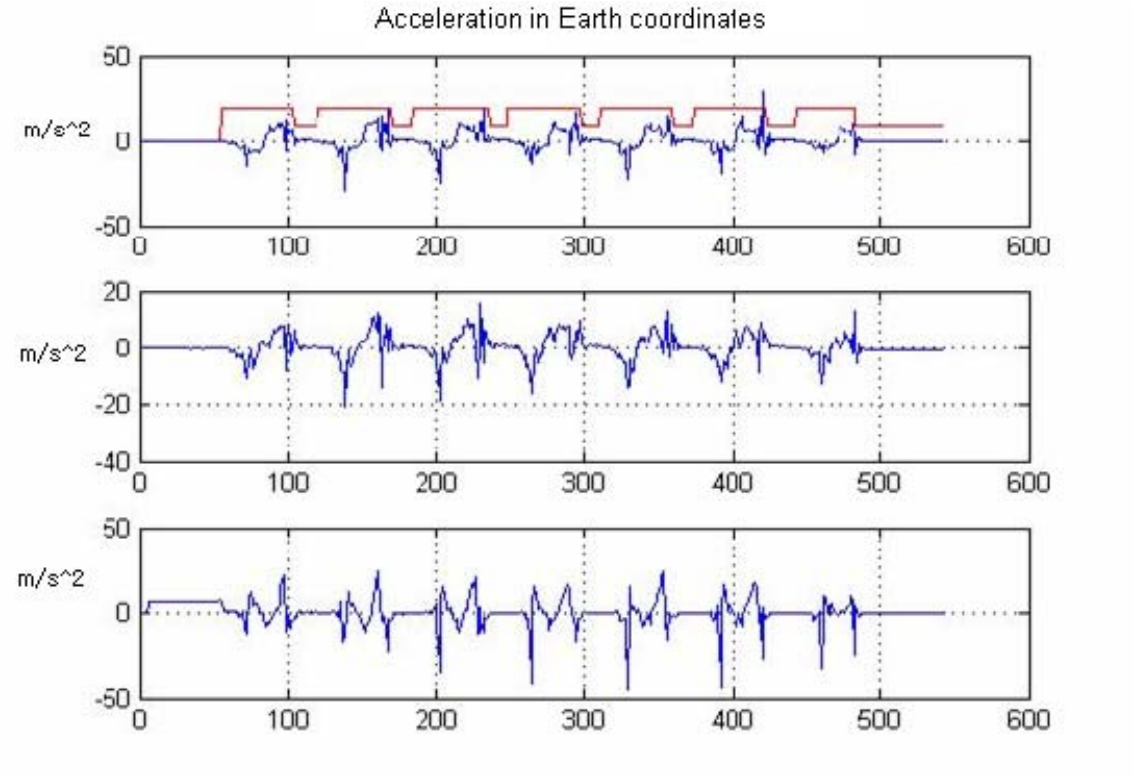

Figure 15. Accelerations after Shifting Windows toward Left Side (X-axis unit is the number of samples and Y-axis unit is meters per the square of seconds).

d. Correction of Acceleration and Velocity

The raw data of acceleration has some errors. During stance phases, the acceleration data should have zero values ideally. However, the real values are not zeros. Figure 16 represents the velocities before any correction. Due to this drift, after integrating the measured accelerations for the velocities, the bigger errors are brought out in the velocities. Thus, it needs a process to correct the values given from the MARG sensor. After determining the gait cycle, the velocities during stance phase were cumulated and then divided by length of stance counts. Then, the average of velocities was subtracted from the velocities when the initial phase was changed into swing phase or stance phase was changed into swing phase. The values from subtracting were called velocity error and then the acceleration errors could be determined. The velocity error was divided by the total sampling time during stance phase. The acceleration errors were

removed at swing accelerations. However, there were errors in the results; the velocities were not zeros at initial time and end time of swing phase.

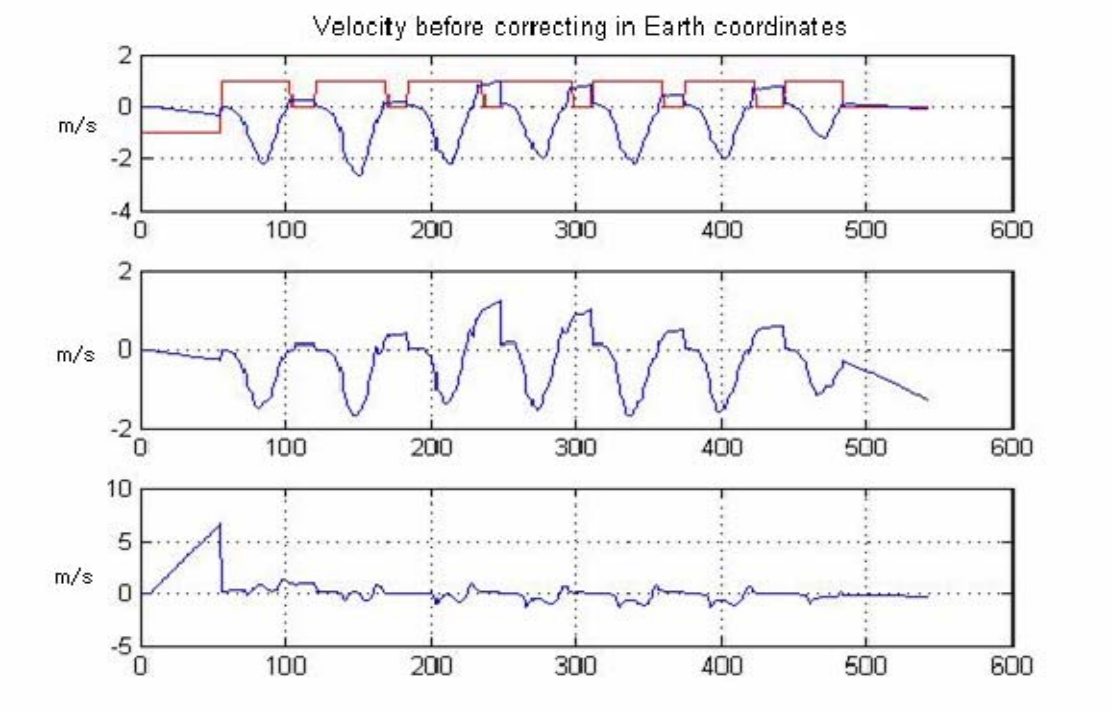

Figure 16. Velocities before Zero Velocity Compensation (X-axis unit is the number of samples and Y-axis unit is meters per seconds).

Thus, during the initial phase, the velocities were compensated as zero values. Moreover, during swing phase, the velocities were corrected by zero velocity compensation using Eq(4. 8).

Before conducting this zero velocity compensation, the distance was longer than measured distance. For example, at 48m walk, the estimated distance was summarized in Table 2.

Date	Experiment #	Step Count	Distance(m)	Threshold	% Error
20.Aug.2007	1	40	51.5266	0.58	7.35
20.Aug.2007	2	40	51.3447	0.58	6.97
20.Aug.2007	3	40	51.6490	0.35	7.60

Table 2. 48m Walks without ZVC.

The error is almost 3m and 7%. This result is not enough to track the human walking. In order to correct this result, the zero velocity compensation method was used.

Figure 17 represents the velocity after the correction. The initial velocity is zero and the start and stop of swing phase are zero.

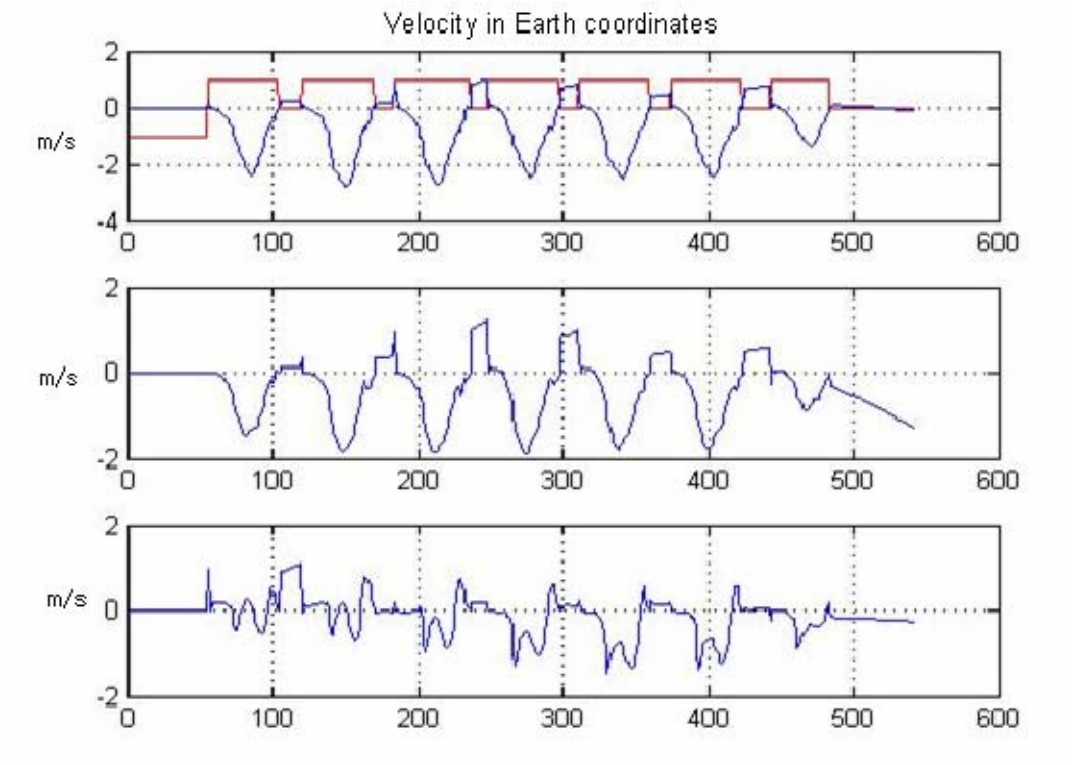

Figure 17. Velocities after Zero Velocity Compensation (X-axis unit is the number of samples and Y-axis unit is meters per seconds).

e. Straight Line Walking Experiments

Several experiments were conducted to determine more accurate distance while walking. Thus experiments of 8m, 16m, 24m, 48m and 150m were conducted at the Naval Postgraduate School. The distances were measured before the experiments using a standard measuring tape. The ground was also determined to be level and sturdy.

The following tables are the results of 8m, 16m and 24m in the Bullard Hall Control Lab. In these experiments, the proper angular rate thresholds were used for the best values. Usually the value was about 0.58.

Date	Experiment #	Step Count	Distance(m)	Threshold	% Error
29.July.2007	1	7	8.0161	0.58	0.2
29.July.2007	2	7	7.8244	0.58	2.195
29.July.2007	3	7	7.9337	0.35	0.83
15.Aug.2007	1	6	7.9337	0.5	0.83
15.Aug.2007	2	6	8.0712	0.58	0.89

Table 3. Results from 8m Walks.

Date	Experiment #	Step Count	Distance(m)	Threshold	% Error
29.July.2007	1	13	14.9214	0.35	6.74
15.Aug.2007	1	13	15.9549	0.55	0.28
15.Aug.2007	2	13	15.9725	0.55	0.17
15.Aug.2007	1	18	23.8433	0.55	0.65
15.Aug.2007	2	19	20.5164	0.58	16

Table 4. Results from 16m and 24m Walks.

A distance of 48m and 150m walks were marked outside of Root Hall on the Naval Postgraduate School campus. A picture of the pathway walked is shown in Figure 18. The 48m walk experiment was done by two people in the same place and at same time. In this case, each person had a unique angular rate threshold. In order to find the best result, several experiments were conducted. As a result it was determined that A's angular rate threshold was about 0.35 and B's angular rate threshold was about 0.58. Table 5 represents the result of these experiments.

Figure 18. Pathway outside of Root Hall at Naval Postgraduate School.

Walker	Date	Experiment #	Step Count	Distance(m)	Threshold	% Error
A	20.Aug.2007	1	40	47.7835	0.54	0.45
A	20.Aug.2007	2	40	46.5809	0.6	2.96
A	20.Aug.2007	3	40	47.7566	0.55	0.5
A	20.Aug.2007	4	40	47.9881	0.58	0.02
B	20.Aug.2007	1	34	48.2712	0.2	0.565
B	20.Aug.2007	2	34	45.4813	0.35	5.25
B	20.Aug.2007	3	33	46.7244	0.4	2.66

Table 5. 48m Walks of two Walkers.

From these results, it could be seen that the walker A's results were better than the walker B's results. The B's step count was 34 and A's step count was 40 so that the B's step was longer than A's. Thus, MARG sensor is better for the walker who has a short step.

In the case of 150m walking, the obtained distance was 149.0796 with 0.43, angular rate threshold with an error of 0.6%. By comparing Table 3, 4 and 5, it could be seen that the outdoor experiments (48m and 150m) were better because the indoor experiments had some disturbances like metal objects. Thus, the magnetometer readings, which are sensitive to the earth's magnetic fields, would be affected by interference from metal objects and result in inaccuracies [1].

f. Stepping and Circular Walking Experiment

Beyond straight line walking, stepping stairs and circular walking were conducted using MARG sensor. The main concept is similar to the straight line walking. However through the same code used for straight line walking, the figures of tracking human movement were not accurate.

In the previous chapter, the human walking was divided as the swing and stance phase. When a person steps stairs upward or downward, the foot also has the stance and swing phase. The period from the time that the foot begins to move into the air to the time that the foot begins to touch the stairs is the swing phase and the period that the foot stays on the stairs is the stance phase. Thus the height would be changed during swing phase periods. In order to calculate the height of the stairs, which the walker stepped, the Z axis acceleration should be integrated two times. However, Z-axis acceleration should be considered as gravity. The gravity is different according to the place because the gravity is influenced by altitude. Thus, in this thesis, the initial value of q(4) (4^{th} quaternion) was subtracted from Z-axis acceleration. The stair case used for this experiment is shown in Figure 19 and experiments were done on 8, October in 2007. This staircase has a turning point in the middle and two stair cases are connected at the same level. The height of the first stair case is 1.92m and the horizontal distance is 2.29m.

The total height of the set of these stairs is 4.46m. The first stair case has 9 steps and second one has 12 steps.

Figure 19. Staircase for Elevation Experiments.

A few tests were done by ascending the first staircase. The experiment was done by two methods, where one method is to ascend the staircase crossing left and right foots. For example, the left foot touched the first step and then the right foot touched the second step and then the left foot touched the third step. The second method is the repeating ascending and pausing. For instance, the left foot touched the first step and the right foot followed the left foot and then the left foot moved toward the second step. Thus, in the first case, the total steps were 5 steps and in the second case, the total steps were 9. A plot of the typical results from this experiment is shown in the following Figures.

Figure 20 represents ascending the first staircase by crossing both feet and Figure 21 shows it in 3 dimensions. Figure 22 represents the walking upward by repeating the ascending and pausing, thus there are 9 stairs in this figure and Figure 23 shows it in 3 dimensions.

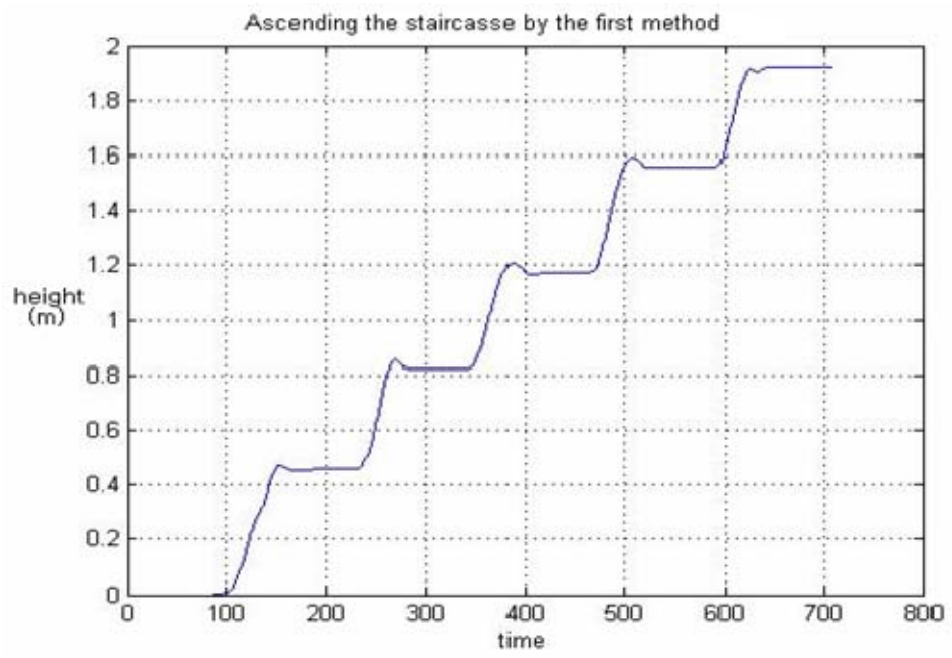

Figure 20. Single Flight of Stairs Experiment by the First method (X-axis unit is the number of samples and height unit is meters).

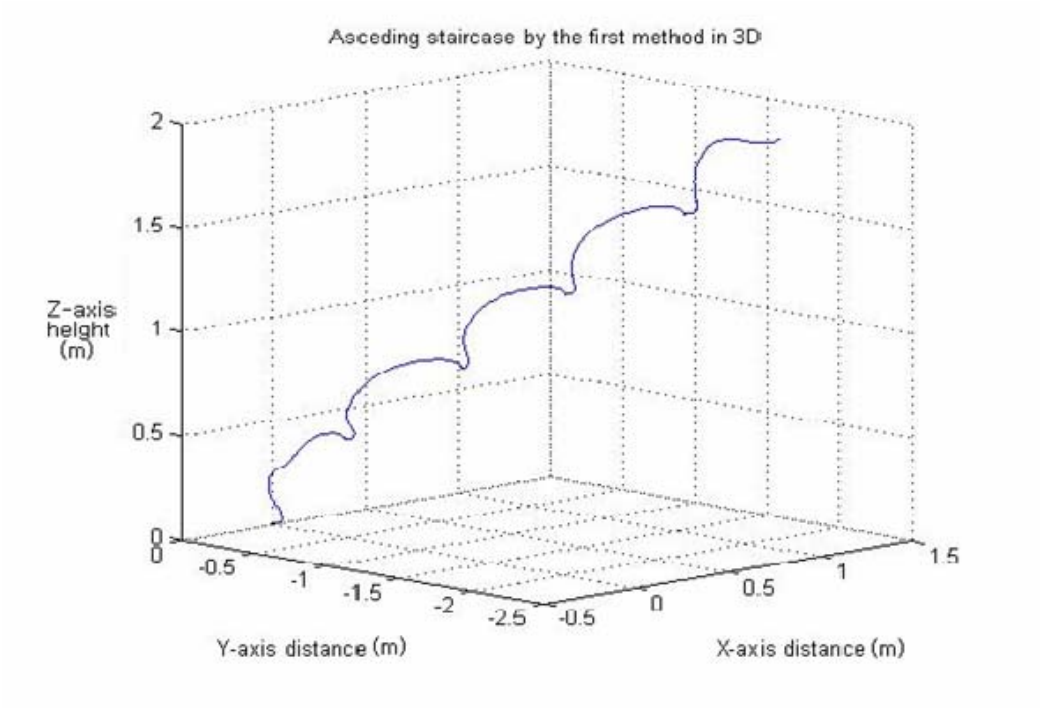

Figure 21. Single Flight of Stairs Experiment by the Second method in 3D (X-axis distance and Y-axis distance units are meters and Z-axis height unit is meters).

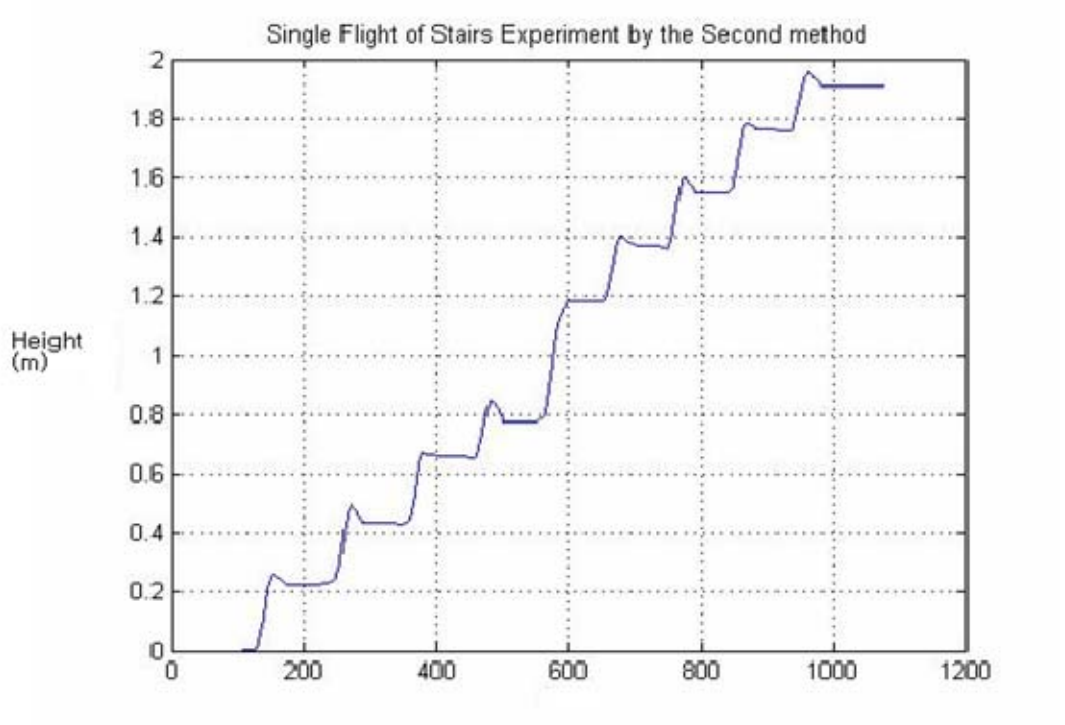

Figure 22. Single Flight of Stairs Experiment by the Second method (X-axis unit is the numbers of samples and height unit is meters).

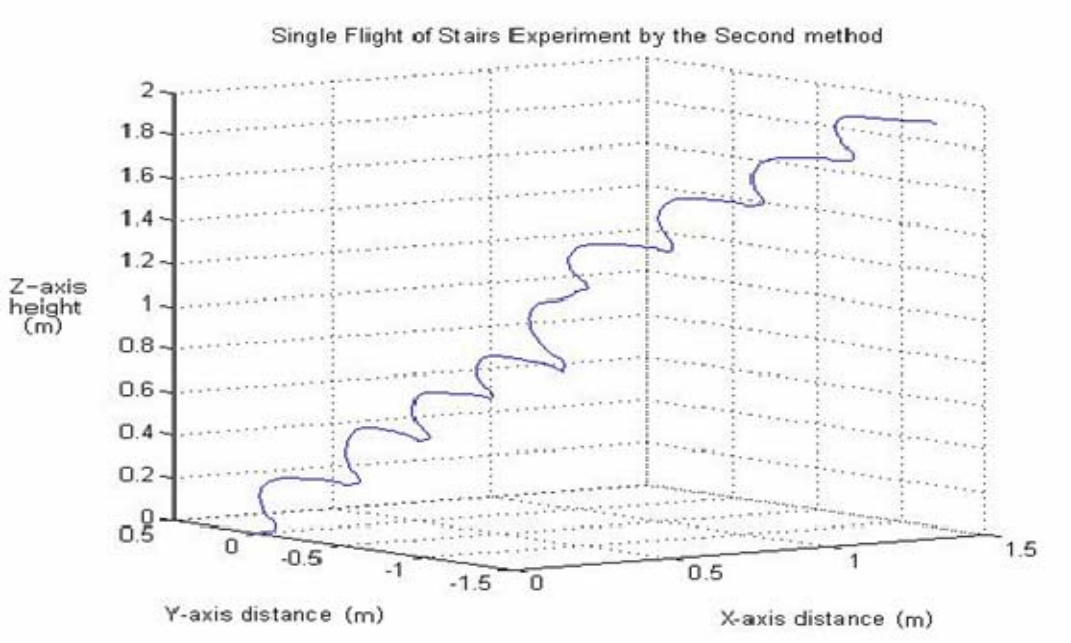

Figure 23. Single Flight of Stairs Experiment by the Second method in 3D (X-axis distance and Y-axis distance units are meters and Z-axis height unit is meters).

Experiment #	Horizontal Distance(m)	Calculated Horizontal Distance(m)	Horizontal %Error	Vertical Distance(m)	Calculated Vertical Distance(m)	Vertical %Error	Threshold
The first method by crossing both foots							
1	2.29	2.3215	1.375	1.92	1.9229	0.15	0.28
2	2.29	2.3714	3.56	1.92	1.9337	0.7	0.33
The second method by ascending as one foot							
1	2.29	1.9646	14.21	1.92	1.9087	0.59	0.28
2	2.29	1.9052	16.773	1.92	1.8624	3	0.33

Table 6. Single Flight Stairs Results.

The results shown in Table 6 are not accurate enough. The calculated vertical distances have the error inside 1%, thus the vertical distance results are encouraging in terms of accuracy. However, the horizontal distance results have a bigger error than the vertical distance results. The horizontal accuracy of MARG sensors appeared to suffer as well while walking up or down stairs.

The next plots show the results of walking up the first flight of stairs, turning at the landing, and then continuing up the rest of the stairs before stopping at the top.

Experiment #	Vertical Distance(m)	Calculated Vertical Distance(m)	Vertical %Error	Threshold
1	4.46	4.3799	1.79	0.33
2	4.46	4.5416	1.83	0.33

Table 7. Double Flight Stair Results.

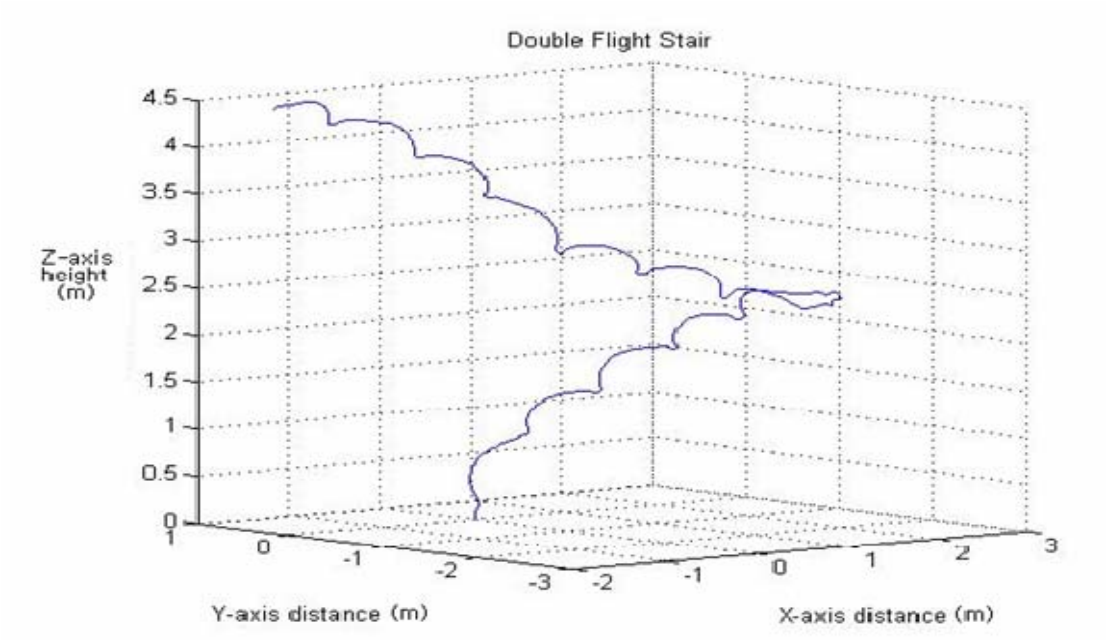

Figure 24. Double Flight Staircase of the First method (crossing foots) (X-axis distance and Y-axis distance units are meters and Z-axis height unit is meters).

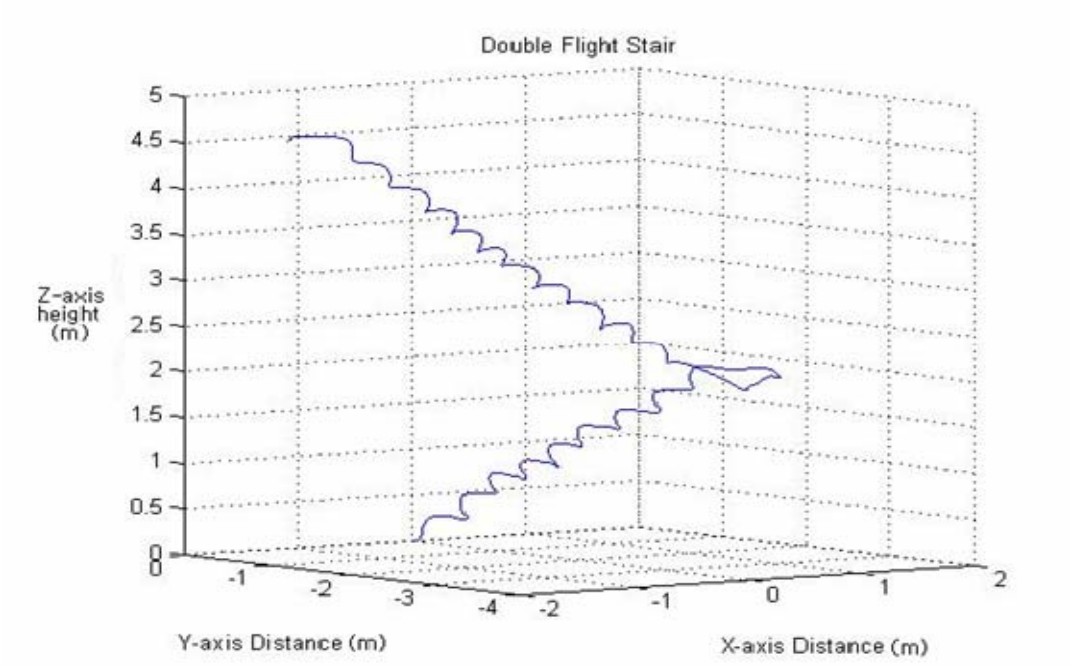

Figure 25. Double Flight Staircase of the Second method (ascending by one foot) (X-axis distance and Y-axis distance units are meters and Z-axis height unit is meters).

The three dimensional plots (Figure 24 and Figure 25) match the real staircase of Figure 19. It can be seen that the vertical distance increases in the Z-axis until about half way, where the walker is turning at the landing before ascending the second flight of stairs. Then the plot increases in the vertical direction until stopping at the top of staircase.

The next experiments were the square walking and the circular walking. The walker started to walk in a straight line before turning 90 degree and then repeated this way until stopping at the same position where walker started. Ideally, the final distance from the starting point to the stopping point should be zero because the position was same and the plot should be square. Furthermore, circular walking also should stop at the initial position. However, the level of accuracy was not encouraging. First, the experiment was conducted in the control lab. The space was small. Experiments #1 and #2 were the results of the square walking and Experiment #3 was the result of the circular walking. These experiments were done at October 3 in 2007 and the angular threshold was 0.55. All of these results did not finish at the initial position. Furthermore, the final position passed the initial position and the figures were not the square. The following figures show the results in X and Y axis dimensions.

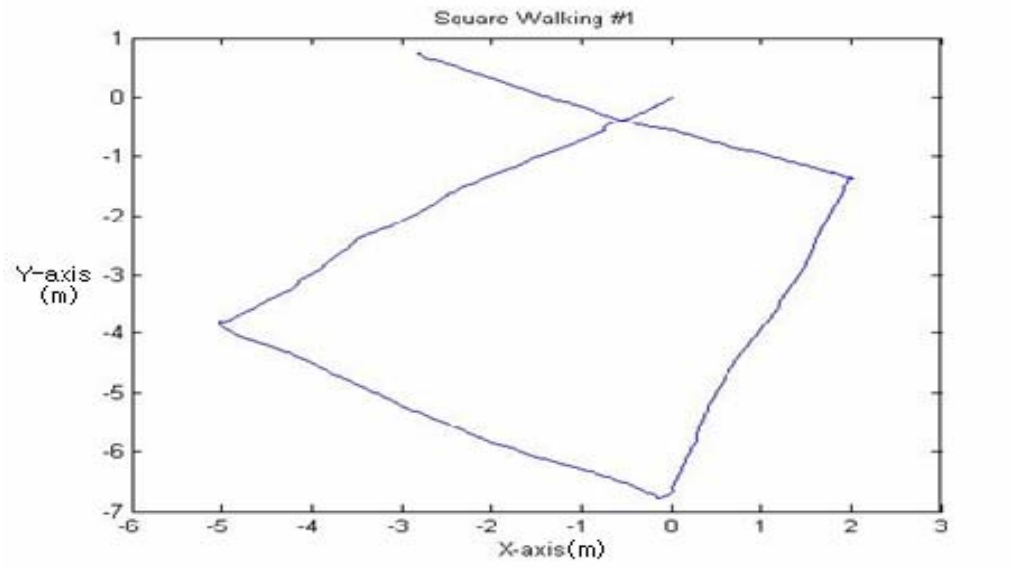

Figure 26. Square Walking Experiment #1 Result (X-axis unit is meters and Y-axis unit is meters).

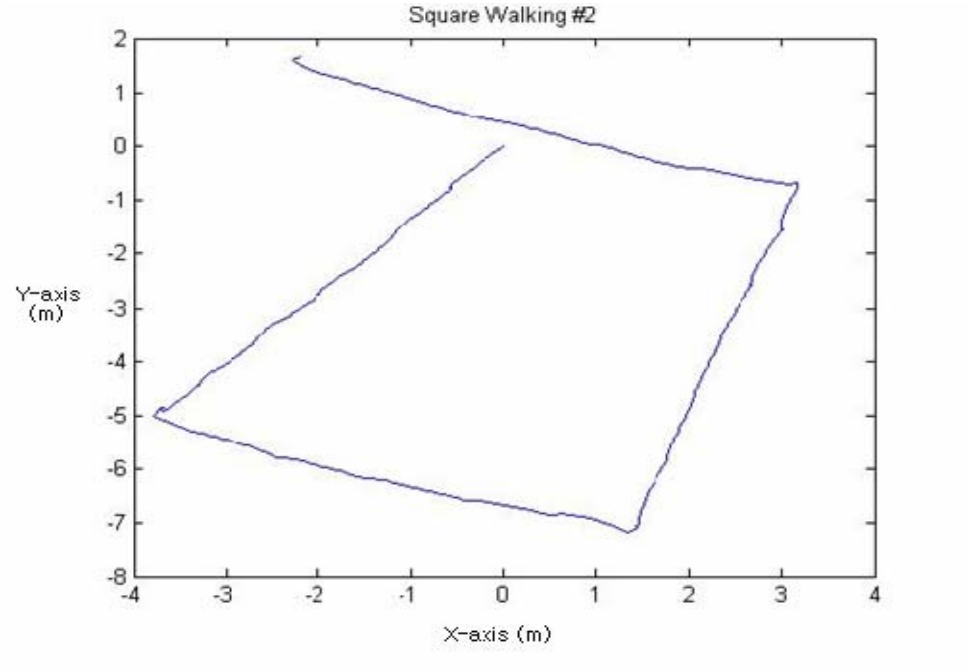

Figure 27. Square Walking Experiment #2 Result (X-axis unit is meters and Y-axis unit is meters).

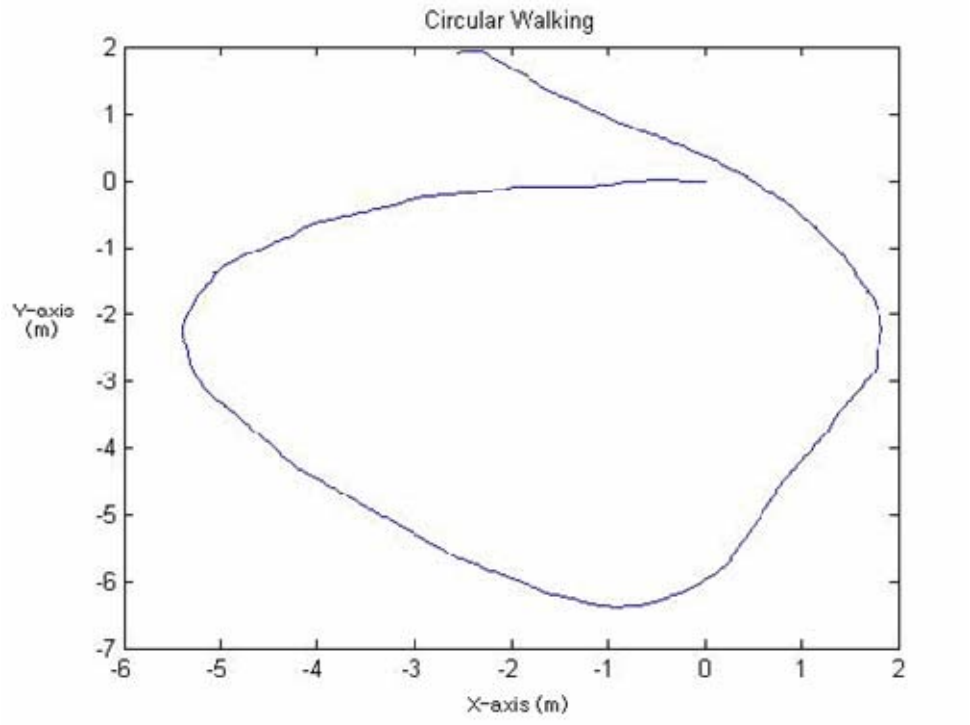

Figure 28. Circular Walking Result (X-axis unit is meters and Y-axis unit is meters).

The next experiments were conducted in the tennis court (Figure 29) of Naval Postgraduate School at October 8, 2007. This place is bigger than the control lab. The way is similar. The walker walked by following the line of court.

Figure 29. Tennis Court for Square Walking.

Figure 30 represents the distance of each X and Y axis of the tennis court walking. And Figure 31 is the result of the tennis court walking in the two dimensional space.

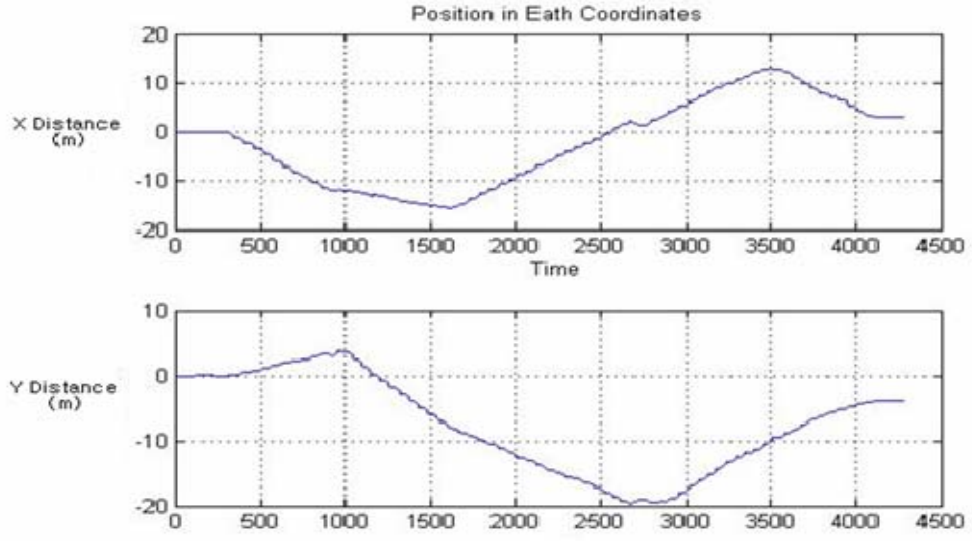

Figure 30. Square Walking Results (X distance and Y distance units are meters and X-axis unit is the number of samples).

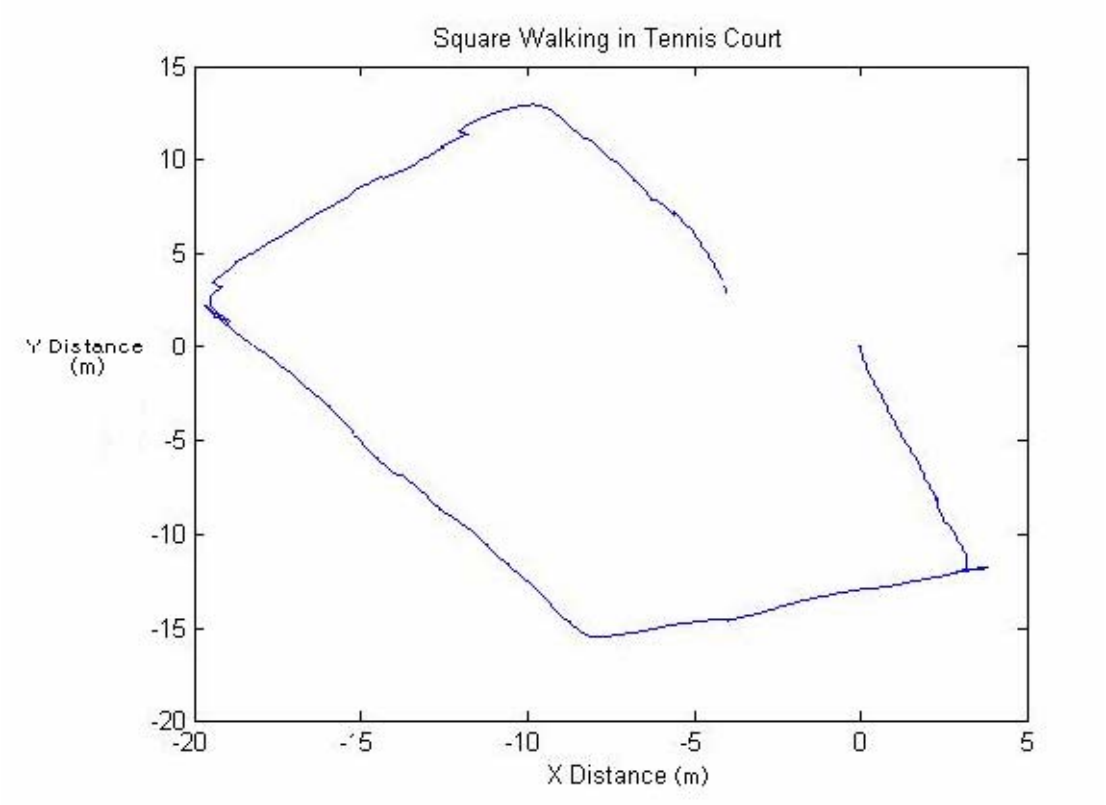

Figure 31. Clockwise Square Walking in the Tennis Court (X distance unit is meters and Y distance unit is meters).

From this result, the square walking in the bigger space was not accurate compared to the smaller place. The final position did not match to the initial position. And the plot was also not an exact square. The following table shows the difference between the starting position and the stopping position through a few experiments in the tennis court.

Date	Experiment #	Difference(m)
Oct 08, 2007	1	7.6182
Oct 08, 2007	2	3.4926
Oct 08, 2007	3	7.4341
Oct 08, 2007	4	5.0103

Table 8. Square Walking Result in the Tennis Court.

The results from these experiments reveal the restriction of MARG sensor's ability to get accurate heading changes. These figures about the position were conducted by integrating X and Y axis accelerations. In these experiments, the angular rate of Z axis was changed because the walker turned the direction. In order to obtain more accurate results, processing to correct the heading is needed. Thus, the next experiments will focus on the correcting the angular rate for the accurate heading.

C. HEADING

1. Background

This part will introduce the heading of human movement. Heading means a direction where a walking person is aiming. In this thesis, two frames were introduced: body frame and earth frame. The body frame is the coordinates of the sensor itself. In order to represent the position of human and the distance, the position vector should be represented in the earth frame. Thus, the data obtained from MARG sensor was transformed by the quaternion. The rotation matrix that was used for transformation was introduced in Chapter III. The MARG sensor measures the three orthogonal accelerations, angular rates and local magnetic field. The earth has magnetism and the magnetometer can measure this magnetism. From the measured data, the direction like North and East can be represented. Thus, the heading can be sensed by these magnetic sensors.

2. Angular Rates for the Heading

Angular rate sensors are used in conjunction with accelerometers to make a dynamic measurement of orientation angles. Angular rate sensors are also used by themselves to track rotational motion. Angular rate is a rotational speed. It is the motion of a record turning on a record player; a pure rotation. Angular rate can be specified in various units:

RPM – rotations per minute

Deg/s – 360deg / 60sec = 60deg / sec

Rad/s – radians per second

1 rad / sec = (180 deg / π rad) * 1 rad/sec = 57.3 deg/sec

A rate sensor can not measure an angle or orientation by itself. It only measures rotational motion. The angular rates can be integrated over time to get angles as a function of time.

$$\theta(t) = \int \omega(t')dt' \tag{4. 9}$$

The next experiment was done at the control lab on October 18th, 2007. The walker walked just 5 steps and then paused for a few seconds and then walked 3 steps again. The data obtained was transformed by the rotation matrix. The angular rates are showing in the Figure 32.

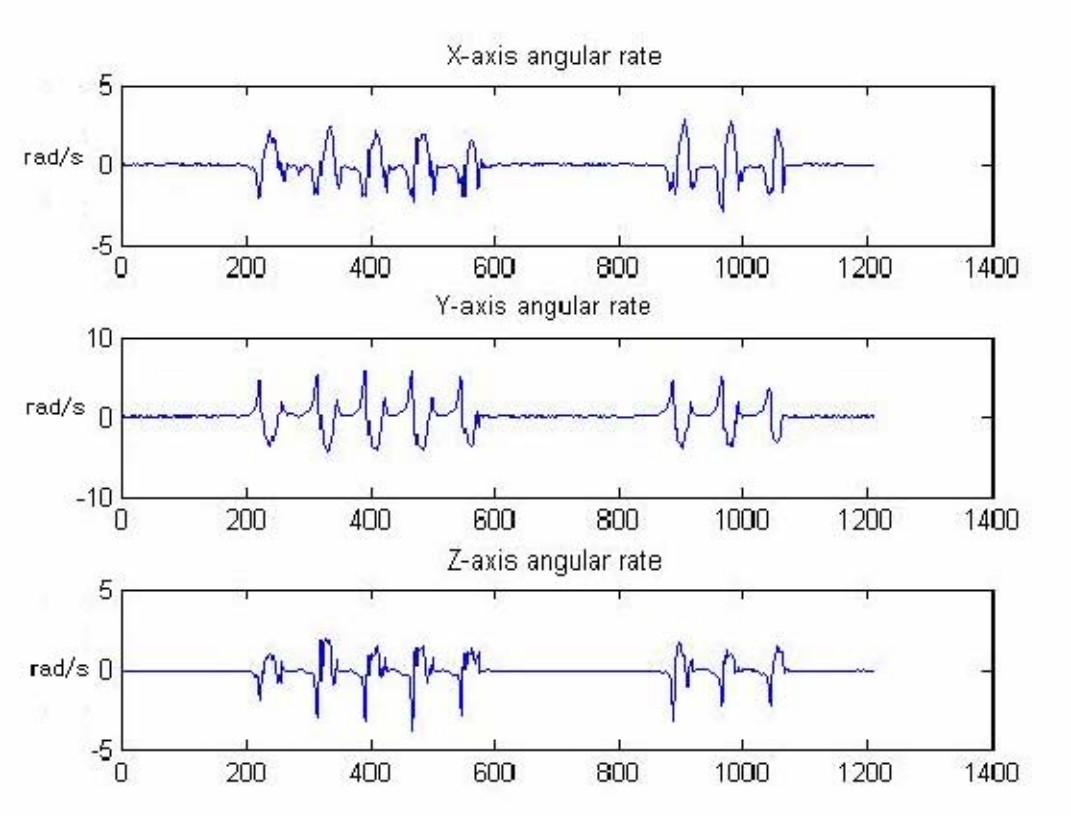

Figure 32. Angular Rates (X-axis unit is the number of sampling and Y-axis unit is radians per seconds).

From these three angular rates, the Z-axis angular rate gives the information about the heading. The angle of each axis was calculated by the integration of the angular rate. Ideally, the angles should not be changed when the walker paused in the same position.

3. Correcting the Angles by Removing Drifts

In Figure 33, the Z-axis angle, yaw increased to about 20 degree at the final position. However the walker did not turn into any direction and just walked a straight line. Thus, the final angle should be a zero degree.

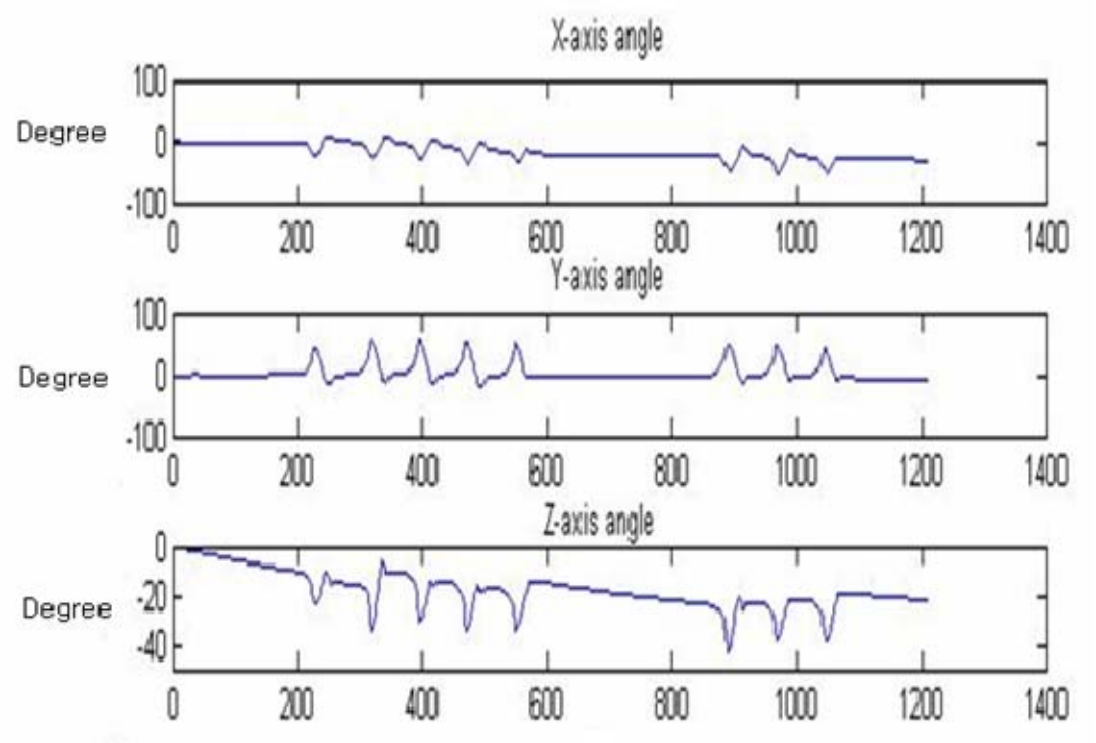

Figure 33. Angles from Original Angular Rates (X-axis unit is the number of samples and Y-axis unit is degrees).

In order to get a more accurate result, some errors require correcting. For the heading, the walking phase was divided into four phases: Initial, Stance, Swing and Turning Swing. The initial phase is determined when the walker does not walk and keeps at the same position for 0.5 seconds or longer. In this experiment, the phase was an initial phase before the first step and the phase was also an initial phase after five steps.

Stance phase is also when the walker touches the land but the time that the walker keeps the same position is shorter than 0.5 seconds. Swing phase is determined when the walker's foot steps out in the air. However, in order to distinguish the swing phase and turning swing phase, the Euler angles were used. The Euler angle could be calculated by Eq(4. 10).

$$\begin{bmatrix} \phi \\ \theta \\ \psi \end{bmatrix} = \begin{bmatrix} \arctan \dfrac{2(q_0 q_1 + q_2 q_3)}{1 - 2(q_1^2 + q_2^2)} \\ \arcsin(2(q_0 q_2 - q_3 q_1)) \\ \arctan \dfrac{2(q_0 q_3 + q_1 q_2)}{1 - 2(q_2^2 + q_3^2)} \end{bmatrix} \tag{4. 10}$$

Figure 34 represents the Euler angles when the walker turned 90 degree after straight line walking. The turning swing phase was determined by the Euler angle of Z-axis. In the figure 34, the Z-axis angle showed a bigger change when the time sample is at about 1150.

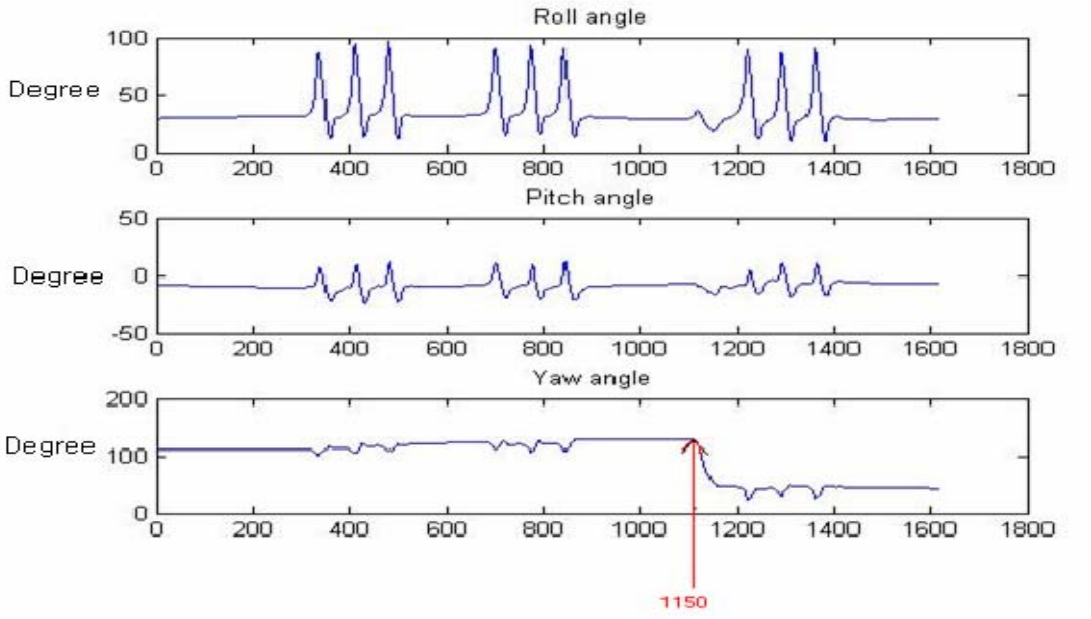

Figure 34. Euler Angles of Turning Walking (X-axis unit is the number of samples and Y-axis unit is degrees).

When the Z axis angle difference had a big value, the section was determined as Turning Swing Phase and the walking phase value was represented as 3.

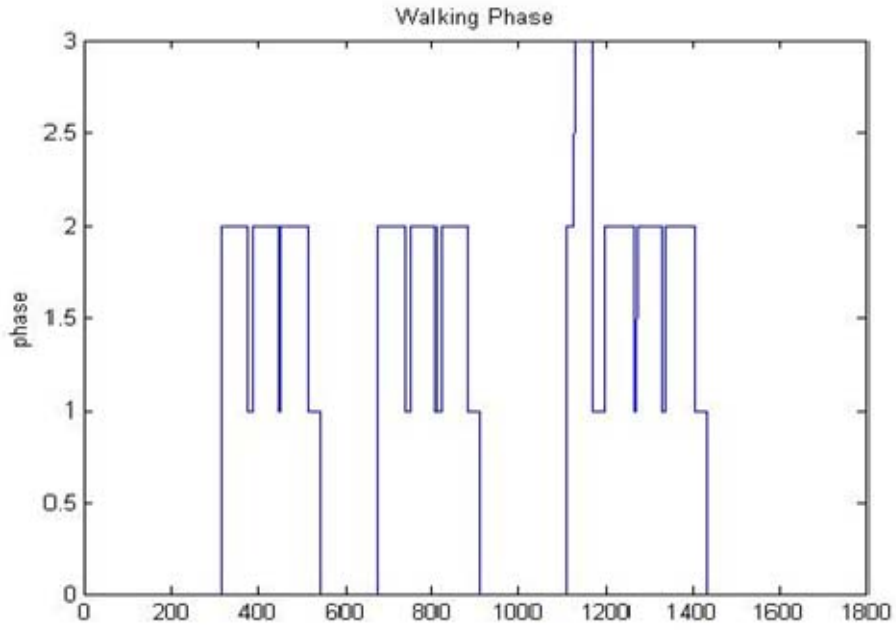

Figure 35. Walking Phase of Turning Walking (X-axis unit is the number of samples and Y-axis unit is constants of walking phase).

From Figure 35, the walker walked 3 steps and paused for a while and then walked 3 steps following the straight line. And the walker kept the same position for a while and then turned 90 degrees and walked 4 steps in the same direction.

In Figure 33, it was known that the sensor had the drift in the angular rates. These drifts were integrated for the angle. Thus, the angle existed during the Stance and Initial phases. In order to find more accurate results, the drift should be removed.

Figure 36 represents the heading angles including the drift. Thus, the angles increased when the walker walked the straight line before the turning point.

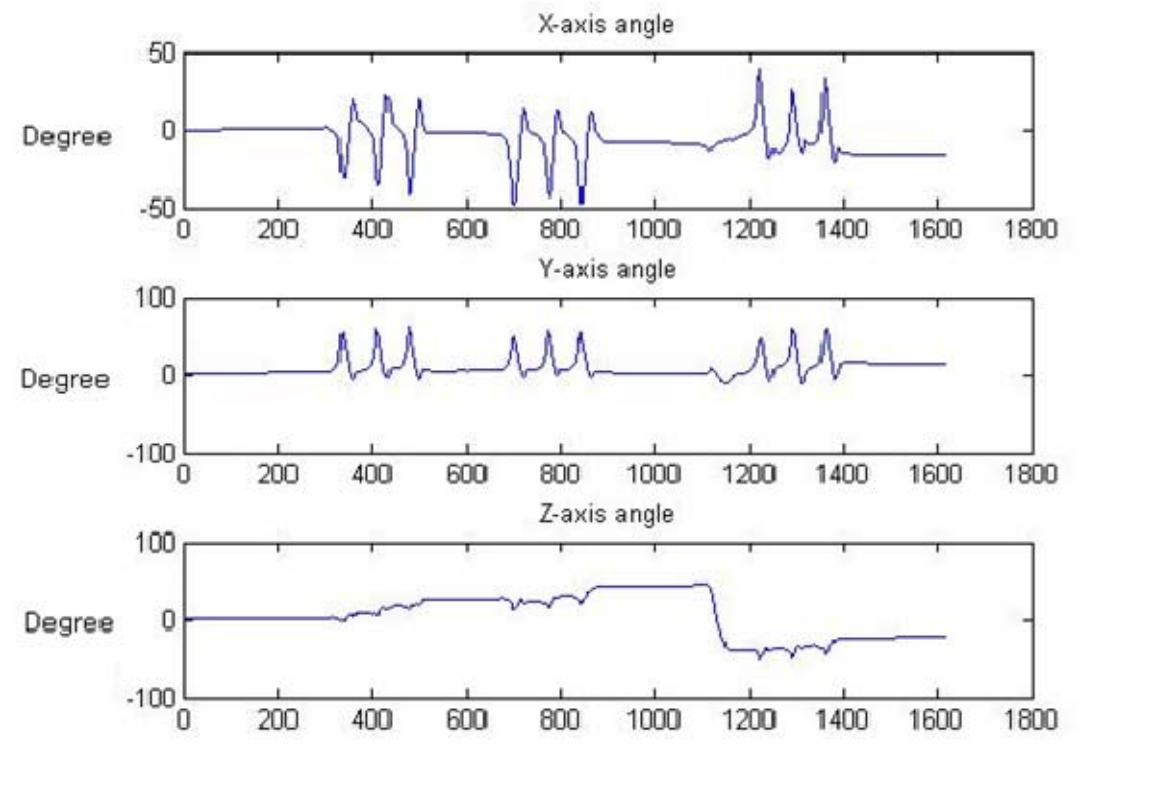

Figure 36. The Angles from the Original Data without Correcting (X-axis unit is the number of samples and Y-axis unit is degrees).

During the Initial phase, the angles should be zero because the walker did not move. Thus, in this case, the angles were corrected as zero value. Moreover, during the stance phase, the angles are assumed as zero values because the walker touched the ground and the foot did not move. However, in this case, the angles were not exact zero values because of the drifts.

$$\begin{aligned} ang'(t) &= \int_{t_0}^{t} (ang\_rate(\tau) + d(\tau))d\tau \\ &= ang(t) + ang\_d(t) \end{aligned} \qquad (4.\ 11)$$

where ang'(t) is the angle from the original data, ang_rate is the angular rate without drifts, d(t) is the drift and ang(t) is the angle without drifts. ang(t) can be assumed that it

has zero values. Thus, the drift can be represented as the average of angles during the Stance phase. The more correct result can be obtained by subtracting this average from the ang'(t).

$$\begin{aligned} ang'(t) &= 0 + ang\_d(t) \\ ang\_d(t) &= mean(ang'(t)) \\ ang(t) &= ang'(t) - mean(ang'(t)) \end{aligned} \qquad (4.\ 12)$$

When the phase was changed from the Swing phase into the Turn Swing phase, the angle would be changed because the walker turned into the other direction. Thus in this point, the obtained angle should be kept.

After these procedures, the more accurate heading result could be obtained as shown Figure 37. The walker turned in a direction of 90 degrees after pausing. Thus the angle was modified as zero value at the turning point and then the angular rates were integrated removing the drifts. Therefore, the final value which the walker stopped to walk was 83.2 degrees.

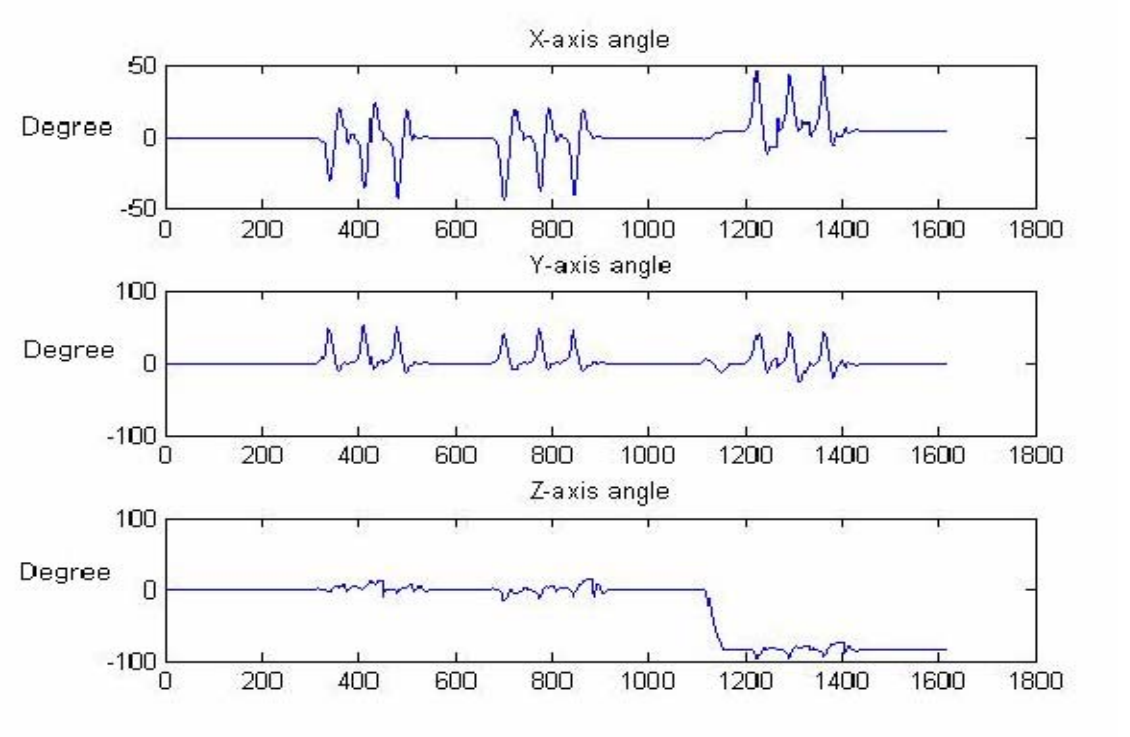

Figure 37. The Result for the Heading after Correcting (X-axis unit is the number of samples and Y-axis unit is degrees).

4. Various Experiments for the Heading

In order to obtain more correct data, various experiments were conducted at the tennis court on October 23, 2007 because the tennis court has the exact square line and is not affected by magnetic interference.

The first experiment was about turning 90 degrees and Table 9 is the result of the first experiment. It was conducted 3 times. The walker walked 3 steps and paused for a while and walked 3 steps more and paused for a while before turning 90 degrees. Thus, at each pausing period, the angle was initialized as zero degree.

Date	Experiment #	Angle(degree)	Threshold	%Error
23.Oct.2007	1	82.2386	0.4	8.624
23.Oct.2007	2	76.6326	0.36	14.85
23.Oct.2007	3	89.3626	0.35	0.71

Table 9. 90 Degree Turning Results.

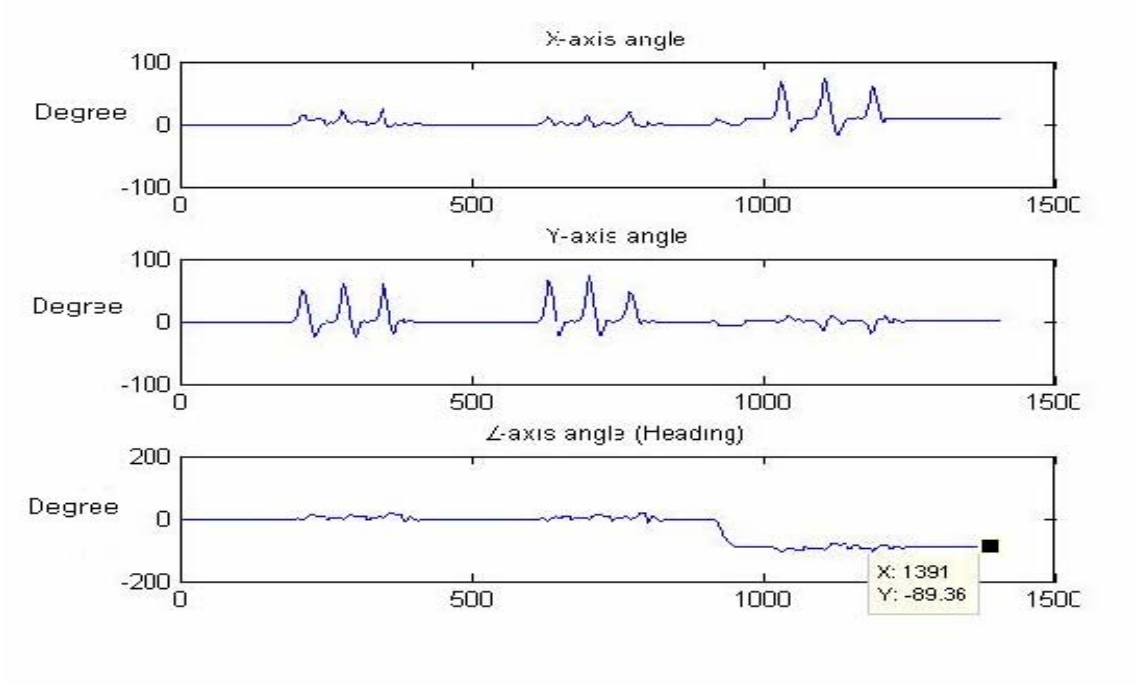

Figure 38. Heading Result of 90 Degree Turn (X-axis unit is the number of samples and Y-axis unit is degrees).

In the first experiment, the final degree had from 76 degree to 89 degree and the error was from 0.71% to 14%. Figure 38 is the result of the experiment #3.

The second experiment was conducted for 180 degree and Table 10 represents the result of the second experiment. The walker turned 90 degree and then turned 90 degree again. Thus, the final heading angle should be 180 degree ideally. This experiment was conducted 4 times. For this experiment, the walker walked as same method of the first experiment until the first 90 degree turning. Then the walker turned 90 degree again after 4 steps. This experiment was also initialized as zero values before turning point.

Date	Experiment #	Angle(degree)	Threshold	%Error
23.Oct.2007	1	163.4721	0.35	9.18
23.Oct.2007	2	153.9947	0.31	14.45
23.Oct.2007	3	163.0901	0.46	9.39
23.Oct.2007	4	174.0096	0.37	3.328

Table 10. 180 Degree Turning Results.

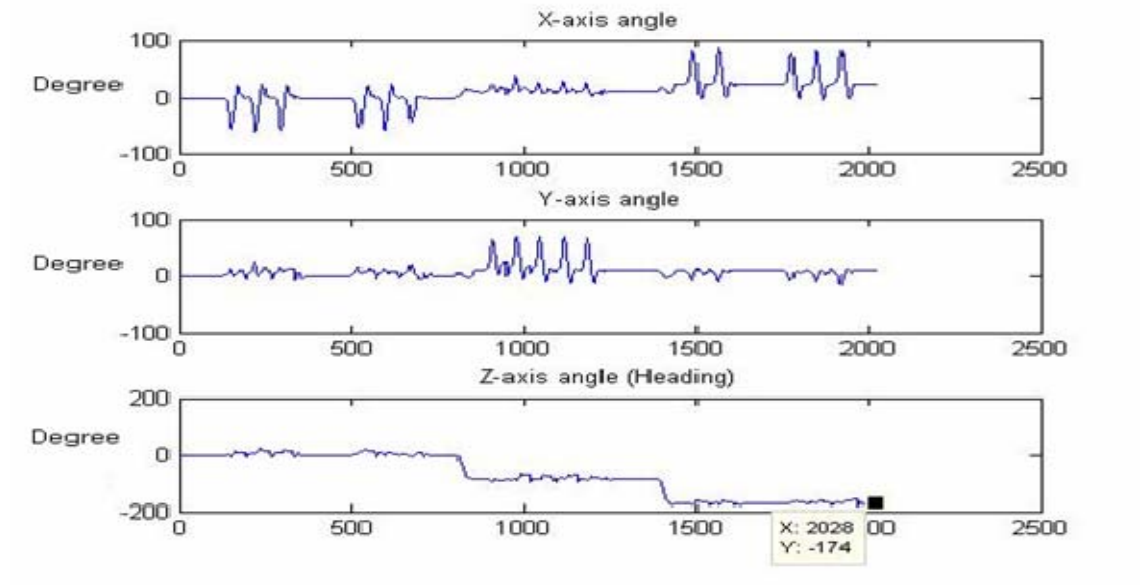

Figure 39. Heading Result of 180 Degree Turn (X-axis unit is the number of samples and Y-axis unit is degrees).

In the second experiment, the final degree had from 153 degree to 174 degree and the error was from 3.3% to 14.45%. Figure 39 is the result of the experiment #4.

In the previous experiments for the distance, the square walking was conducted. However, the figures were not an exact square and the heading was different. In order to obtain a more correct result, the heading angle should be modified. In the final experiment, the walker walked following the square line and Table 11 is the result of the final experiment. This experiment was conducted 3 times. The experiment #1 and experiment #2 of the final experiment were conducted in the same way. The walker paused for a second at the each turning point. However, the last one was conducted without pausing time at the turning point. Ideally, at the end position, the heading angle should be 360 degree. However, the estimated angles were from 341.5 degree to 354.4 degree and the error was from 1.55% to 5.14%.

Date	Experiment #	Angle(degree)	Threshold	%Error
23.Oct.2007	1	341.4788	0.33	5.14
23.Oct.2007	2	343.4425	0.36	4.6
23.Oct.2007	3	354.4059	0.35	1.55

Table 11. 360 Degree Turning Results.

Figure 40 is the heading angle result of the experiment #2. This was conducted with the initializing at the pausing point because the walker paused for a while before tuning into the other direction. Figure 41 is the heading angle of experiment #3. From this figure, it was seen that the result did not have the initial phase during walking because the walker did not paused before turning. Thus this heading result was not modified as zero values before turning. However, during stance and swing phases, the angle was corrected by removing the drift. Thus the result was also corrected.

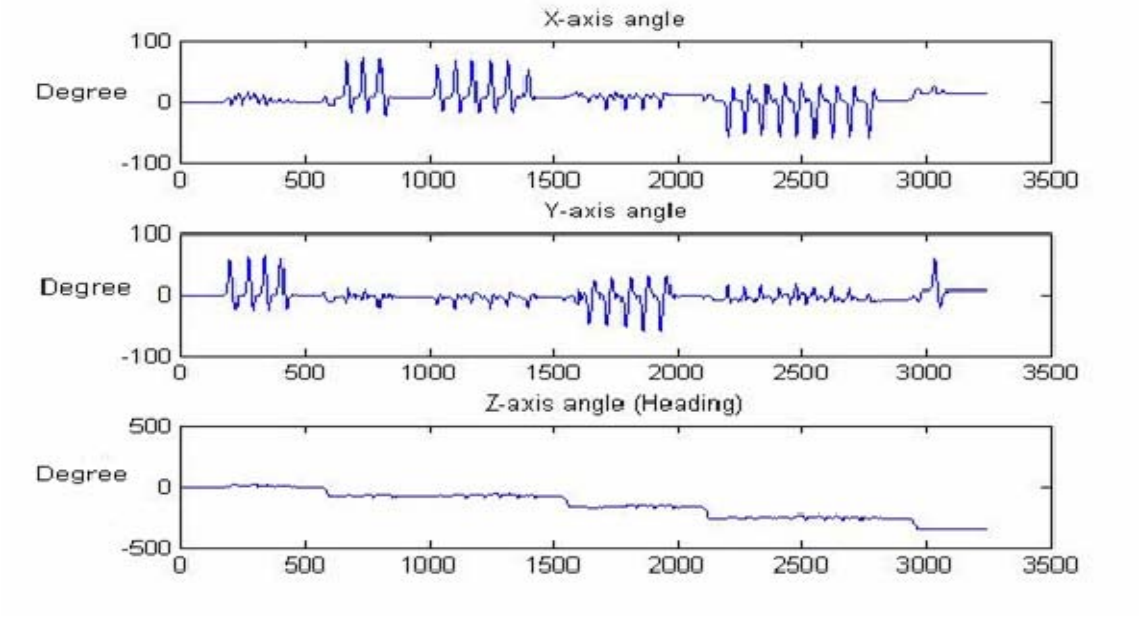

Figure 40. 360 Degree Heading with Initializing (X-axis unit is the number of samples and Y-axis unit is degrees).

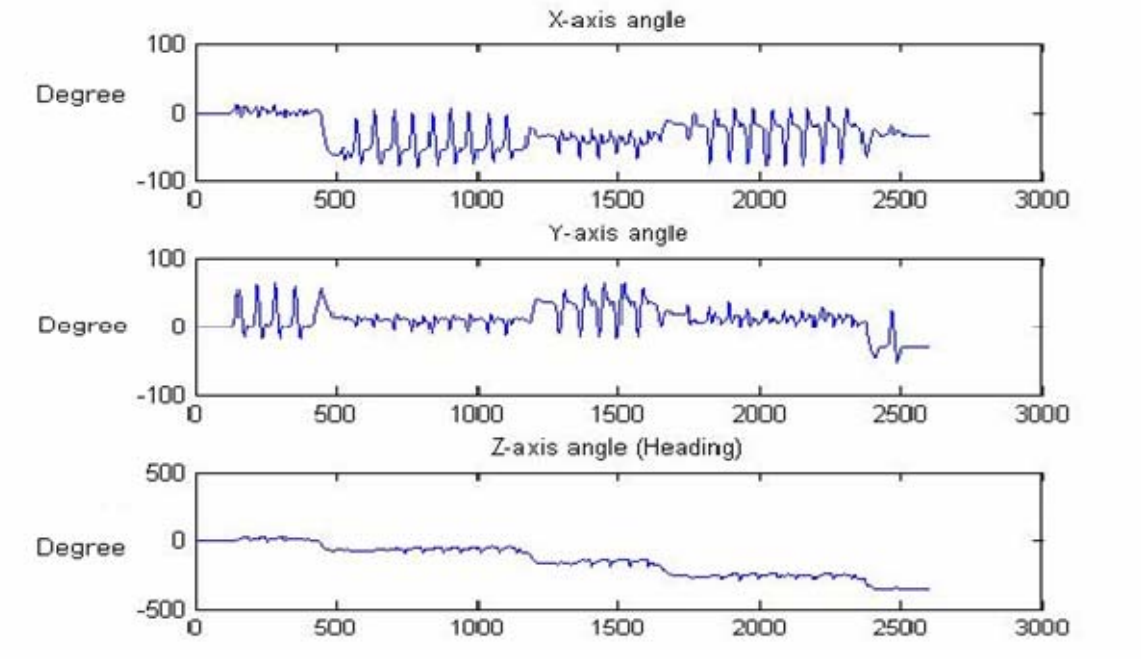

Figure 41. 360 Degree Heading without Initializing (X-axis unit is the number of samples and Y-axis unit is degrees).

D. SUMMARY

This chapter presented the experimental results about straight walking, stepping and square walking. The three-dimensional position in the X, Y, and Z directions was obtained by integrating three-dimensional acceleration measurements twice. To improve the position accuracy, a drift correction was applied to the measured acceleration based on the gait cycle.

Heading computed from magnetometer data was determined to be less accurate. An alternative method for computing heading was used. It was based on angular rate data. A similar drift correction based on the gait cycle was applied to angular rate data. The results are encouraging, although more experiments are needed to improve the tracking accuracy.

THIS PAGE INTENTIONALLY LEFT BLANK

V. CONCLUSIONS AND FUTURE WORK

A. CONCLUSIONS

There have been ongoing efforts to track the human motion in a real time virtual environment. This thesis has extended that research in several ways.

For the walking distance, the acceleration was integrated twice. However, the distance was not accurate because the acceleration from the sensor had a drift. In order to remove the drift, the velocity obtained by integrating the acceleration was used. The velocity was corrected based on the fact that the foot velocity is zero during the stance phase. The corrected velocity was integrated to determine total displacement.

While the results for straight walking are acceptable, the results for square or circular walking are less accurate due to large heading errors. The Z component of angular rates was integrated to obtain the heading angle. Prior to integration, a similar drift correction based on the gait cycle was applied to angular rates.

In this thesis, several experiments were performed using the MARG sensor which was placed on a person's foot. In order to determine the distance, the first experiment was conducted with a straight line walking of various distances (8, 24, 48, and 150 meters). The second experiment was done with walking up a flight stairs to determine the height. The last experiment was conducted with a square pattern walking. In order to obtain various heading angles, the experiment was done with various degrees (90, 180, and 360 degrees).

B. FUTURE WORK

In this thesis, the displacement and heading experiments were conducted separately. However, in order to track the human movement of walking in a square pattern, the corrected heading should be connected with the displacement. Thus, a combined treatment will be needed for the more accurate result in the future.

As compared with the displacement error, the heading error was bigger. Thus, for more accurate heading result, better drift correcting procedures will be needed. Further

research is needed to better characterize the drift found in the sensor data. In this project, the drift was removed just using the average of the obtained data during the stance phase. The drift appears to have the same properties as a random walk, yet there has not been enough research to model the drift. Future work will need to analyze the drift more. Zero velocity compensation was used to correct the drift error in the accelerometers. This algorithm assumes the accelerometer error model was linear in velocity. The acceleration is updated backwards at the end of each step. Hence, more experimental effort is required to analyze the drift error model for the accelerometer.

In order to calculate the height of stairs, Z component acceleration was used. Z component acceleration was integrated twice to obtain the height. Before integrating, the gravity was subtracted. However the gravity is different from place to place. In this thesis, a constant was used. Future work needs to determine it at the every place.

A better stance/swing phase detection is important. In this thesis, the angular rate magnitude of X and Y components was used. The threshold is different from person to person. Future research needs to determine the threshold for each person in real time.

LIST OF REFERENCES

[1] Hyatt Moore IV, *Networked humanoid avatar driven by MARG sensors*, Master's Thesis, Naval Postgraduate School, Monterey, California, September 2006.

[2] T. Starner D. Kirsh and S. Assefa, *"The locust swarm: An environmentally-powered, networkless location and messaging system,"* Proceeding of the First International Symposium on Wearable computers, pp. 169-170, October 1997.

[3] Yilun Luo, *An Attitude Compensation Technique for a MEMS Motion Sensor Based Digital Writing Instrument*, Master's Thesis, Chinese University, Hong Kong, August 2006.

[4] Ionnis Pantazis, *Tracking Human Walking Using MARG Sensors*, Master's Thesis, Naval Postgraduate School, Monterey, California, June 2007.

[5] *Joint Function and Gait analysis,* Instructional Course Lectures, Online reference:http://www.wings.buffalo.edu/academic.department/eng/mae/course/417-517/Orthopaedic%20Biomechanics/lecture%204.pdf (last viewed on October 22, 2007).

[6] *kinematic analyses of gait*, Instructional Course Lecture, Online reference: http://moon.ouhsc.edu/dthompso/gait/knmatics/gait.html (last viewed on October 22, 2007).

[7] Segawa Koichi and Inooka Hijaru, *"Non-restricted Measurement of Walking Distance,"* Proceedings of the 2000 IEEE International conference on Systems, Man and Cybermetics, Nashvill, Taiwan, pp1847-1852, October 2000.

[8] Xiaoping Yun, Eric R. Bachmann, Hyatt Moore IV, and James Calsudian, *"Self-contained Position Tracking of Human Movement Using Small Inertial Magnetic Sensor Modules,"* proceeding of the 2007 IEEE Internetional Conference on Robotics and Automation, Roma, Italy, pp. 2526-2533, April 2007.

[9] MicroStrain, Inc., Technical Product Overview: 3DM-GX1 Gyro, Enhanced Orientation Sensor, 2005, Online reference: http://www.microstrain.com/3DM-GX1.ASPX (last viewed on October 22, 2007).

[10] Jack B. Kuipers, Quaternions and Rotation Sequences, Princeton University Press, 1999.

[11] MicroStrain, Inc., 3DM-G Adapter software Document, May 06, 2003.

[12] MicroStrain, Inc.,3DM-G Data Communication protocol, February 17, 2005.

INITIAL DISTRIBUTION LIST

1. Defense Technical Information Center
   Ft. Belvoir, Virginia

2. Dudley Knox Library
   Naval Postgraduate School
   Monterey, California

3. Professor Xiaoping Yun
   Naval Postgraduate School
   Monterey, California

4. Professor Peter Ateshian
   Naval Postgraduate School
   Monterey, California

5. James Calsudian
   Naval Postgraduate School
   Monterey, California